Anomalous diffusion, nonergodicity, non-Gaussianity, and aging of fractional Brownian motion with nonlinear clocks

Yingjie Liang [1,2,*] Wei Wang [2,†] Ralf Metzler [2,3,‡] and Andrey G. Cherstvy [2,§]
[1] *College of Mechanics and Materials, Hohai University, 211100 Nanjing, China*
[2] *Institute of Physics and Astronomy, University of Potsdam, 14476 Potsdam, Germany*
[3] *Asia Pacific Center for Theoretical Physics, Pohang 37673, Republic of Korea*

(Received 17 April 2023; accepted 7 August 2023; published 13 September 2023)

How do nonlinear clocks in time and/or space affect the fundamental properties of a stochastic process? Specifically, how precisely may ergodic processes such as fractional Brownian motion (FBM) acquire predictable nonergodic and aging features being subjected to such conditions? We address these questions in the current study. To describe different types of non-Brownian motion of particles—including power-law anomalous, ultraslow or logarithmic, as well as superfast or exponential diffusion—we here develop and analyze a generalized stochastic process of scaled-fractional Brownian motion (SFBM). The time- and space-SFBM processes are, respectively, constructed based on FBM running with nonlinear time and space clocks. The fundamental statistical characteristics such as non-Gaussianity of particle displacements, nonergodicity, as well as aging are quantified for time- and space-SFBM by selecting different clocks. The latter parametrize power-law anomalous, ultraslow, and superfast diffusion. The results of our computer simulations are fully consistent with the analytical predictions for several functional forms of clocks. We thoroughly examine the behaviors of the probability-density function, the mean-squared displacement, the time-averaged mean-squared displacement, as well as the aging factor. Our results are applicable for rationalizing the impact of nonlinear time and space properties superimposed onto the FBM-type dynamics. SFBM offers a general framework for a universal and more precise model-based description of anomalous, nonergodic, non-Gaussian, and aging diffusion in single-molecule-tracking observations.

DOI: 10.1103/PhysRevE.108.034113

I. INTRODUCTION

A. Background and motivation

The paradigmatic drift-free Brownian motion (BM) [1–7] features a Gaussian linear-in-time ergodic [8] spreading dynamics of test particles. BM is omnipresent in a multitude of rather simple interaction-free memoryless stationary physical systems of thermally agitated passive monodisperse tracers. The mean-squared displacement (MSD) for BM is

$$\langle x^2(t)\rangle = 2K_1 t^1 \tag{1}$$

and BM is ergodic in the Boltzmann-Birkhoff-Khinchin sense [9–11]. The latter means that the long-time average of a statistical observable converges to its ensemble-based average [11,12]. BM is nonaging in the sense of independence of statistical observables on the observation time T [12–14].

The central quest in analyzing ever-more-detailed experimental data from single-particle-tracking (SPT) assays [15,16] is to pinpoint the precise underlying physical stochastic process and confidently predict its associated parameters [17–20]. Single-parameter BM is, however, often insufficient for a satisfactory, parameter-sensitive, and robust-to-"perturbations" description of rich experimental data. The latter stem from complex real-world systems, driven by processes with sometimes intricate long-ranged physicochemical interactions, multilevel couplings, interdependencies of parameters, memory functions, time-space variabilities, ensemble heterogeneities, polydispersity in the properties of particles, etc. These complications inevitably necessitate a theoretical development of more sophisticated, tunable, and predictive stochastic models, which are generally non-Brownian, non-Gaussian, nonergodic, and aging. Such a development is the main motivation of the current study.

B. Anomalous diffusion

Anomalous diffusion processes [14,18,19,21–31] featuring a nonlinear-in-time (non-Fickian [2] or non-Brownian [1]) growth of the MSD have been widely observed over the last couple of decades, ranging from superdiffusive cosmic-ray propagation in the interstellar medium [32] on the galactic scale [33–35] to subdiffusion of nanometer-sized tracers inside biological cells on the submicron scale [36–39] and to short-time superdiffusion of vortices in ultraquantum turbulence in superfluid helium-4 [40], to motion a few examples.

Physically, the MSD growth of the power-law form [14,25]

$$\langle x^2(t)\rangle = 2K_\rho t^\rho, \tag{2}$$

where K_ρ is the generalized diffusion coefficient (with the dimensions length^2/time$^\rho$) and ρ is the anomalous scaling exponent, describes the regimes of subdiffusion (for $0 < \rho < 1$), BM ($\rho = 1$) [1,3–6], superdiffusion ($1 < \rho < 2$),

*liangyj@hhu.edu.cn
†weiwangnuaa@gmail.com
‡rmetzler@uni-potsdam.de
§a.cherstvy@gmail.com

TABLE I. Some important and experimentally accessible properties (abbreviations used are Y = Yes and N = No) of some pure and hybrid SBM- and FBM-related stochastic processes. We present Fickianity in the sense of short-time linearity of the MSD and mean TAMSD, stationarity for the increment process, ergodicity in the sense of MSD=TAMSD equivalence for long trajectories, Markovianity as the absence of memory effects for consecutive particle's displacements, Gaussianity of the probability-density function (PDF) form, and aging as a TAMSD dependence on the trajectory length T. Note a transition of all diffusion properties being standard for processes on the top to all "canonical" postulates being violated for processes on the bottom of the table.

Processes ↓ Properties →	Fickianity (MSD)	Fickianity (TAMSD)	Stationarity	Ergodicity	Markovianity	Gaussianity	Nonaging
BM [1,3,5]	Y	Y	Y	Y	Y	Y	Y
FBM [54,55]	N	N	Y	Y	N	Y	Y
SBM [56,57]	N	Y	N	N	Y	Y	N
HDP [58,59]	N	Y	N	N	Y	N	N
FBM-HDP [60]	N	N	N	N	N	N	N
SBM-HDP [61]	N	Y	N	N	Y	N	N
FBM-SBM [62]	N	N	N	N	N	Y	N
Time-SFBM, Sec. II	N	N	N	N	N	Y	N
Space-SFBM, Sec. III	N	N	N	N	N	N	N
Time-space-SFBM, Sec. IV	N	N	N	N	N	N	N

ballistic motion ($\rho = 2$), and hyperdiffusion (or superballistic motion [41], with $\rho > 2$). Nonlinear forms of the MSD growth with time [Eq. (2)] are related to *non-Fickianity* or *non-Brownianity* of diffusion. Other functional forms of anomalous diffusion proposed and detected include the ultraslow [42,43] logarithmic and the superfast [44] exponential growth of the MSD. The first case is a part of the class of Sinai-type [45] diffusion, while the second scenario is realized, e.g., for the speculative growth [46–53] of stock-market indices. Note that an adequate and balanced referencing even to the most representative examples of anomalous-diffusion observations from various domains of physics, chemistry, and biochemistry is beyond the scope of this study.

C. Relevant stochastic anomalous-diffusion processes

The description of non-Brownian and non-Gaussian diffusion processes is often a challenging task in situations when the underlying physical mechanism and the associated stochastic model are to be extracted from data and justified. A number of frameworks and stochastic processes (see Table I) have been proposed in the statistical-physics community to unravel the properties of anomalous-diffusion processes, defining a subset of general processes satisfying Eq. (2). The list includes continuous-time random walks (CTRWs) [14,63–65], diffusion on fractals [23], fractional BM (FBM) [54,55] (see also recent Refs. [30,66–75]), concentration-dependent diffusion of power-law form [76,77], multistate diffusion (e.g., with stochastically changing diffusivities [78] and scaling exponents [38]), diffusing-diffusivity-based models [69,70,79–85], annealed transit-time models [19,86,87], heterogeneous diffusion processes (HDPs) [58,59,88–93], scaled BM (SBM) [56,94–97], diffusion in expanding media [98–101], and many other models [including geometric BM (GBM) [46,47,50,51,102] featuring the exponential MSD].

Let us shortly introduce a set of anomalous-diffusion models of a particular interest as mathematical frameworks that will be generalized by stochastic processes invented in the current study. The model of subdiffusive CTRWs [14] is nonergodic [103], being often used to capture the anomalous spreading of particles featuring long-tailed waiting-time and/or jump-length distributions. *Nonergodicity*—a concept first introduced by Boltzmann [8] and developed by, among others, Birkhoff, von Neumann, and Khinchin [9–11]—is defined hereafter as the nonequivalence of ensemble- and time-based averaging [14,104,105]; namely, in the limit $\Delta \ll T$,

$$\langle x^2(\Delta)\rangle \neq \overline{\delta^2(\Delta)}. \tag{3}$$

It thus describes the situations when the MSD (2) is not equal to the long-observation-time time-averaged MSD (TAMSD) defined for a single trajectory as [14]

$$\overline{\delta^2(\Delta)} = \frac{1}{T-\Delta}\int_0^{T-\Delta}[x(t+\Delta)-x(t)]^2 dt. \tag{4}$$

Here T is the trajectory length and Δ is the lag time.

Similarly nonergodic (also quantitatively, as assessed in Ref. [59]) is the HDP [58,59,88,90], emerged based on several "classical" considerations of position- and/or concentration-dependent diffusion (see Refs. [106–110]). In its standard formulation, HDPs describe power-law-type anomalous diffusion in heterogeneous media with a position-dependent power-law-like diffusion coefficient, $D(x) \propto |x|^\beta$ [58,59,88,90], used, e.g., as a model of deterministically varying porosity, of dispersion in nonequilibrium systems with a temperature gradient, or of diffusion in quasi-one-dimensional channels with a variable cross section [111,112]. The "exponential" HDP gives rise to ultraslow diffusion for an exponential spatial dependence of the diffusivity $D(x) \propto e^{-\bar{\lambda}x}$, namely, $\mathrm{MSD}(t) \propto \log^2(t/\tau(\bar{\lambda}))$ [88], and to GBM-like motion for $D(x) \propto x^2$ (this dependence is a critical point [59,110] of the power-law $D(x)$ variation). The process of logarithmic HDP with logarithmically dependent diffusivity was also studied [88]; $D(x)$ e.g. exponentially decaying in space [88] were used; for instance, to describe bombardment- [113] and irradiation-enhanced [114] diffusion. Recently, the theory of confined [89,93] and reset [115] HDPs was developed.

The process of SBM also describes nonergodic anomalous diffusion [56,57,94,116,117]. SBM is an inherently nonstationary memoryless Markovian stochastic process applicable to diffusion in aging or accelerating systems with, e.g., a time-varying temperature. The property of *Markovianity* means that

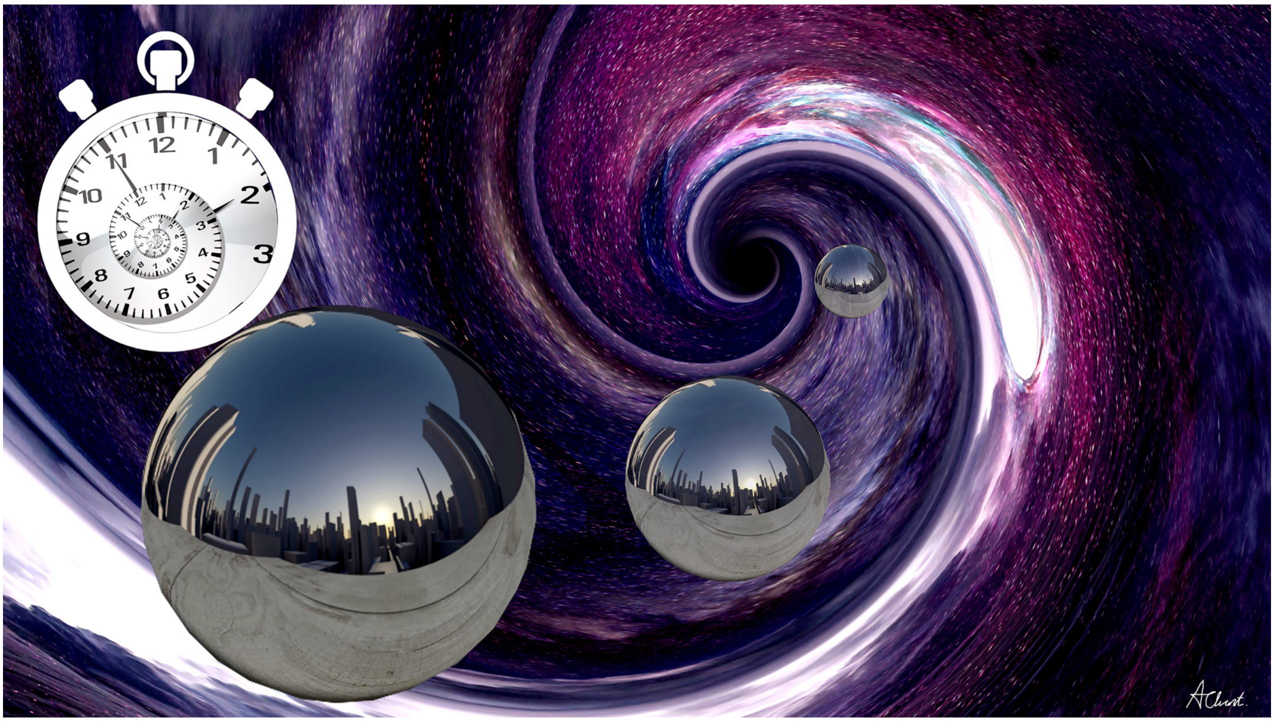

FIG. 1. Artistic representation of nonlinear time and space clocks running for the process of SFBM [175].

the value of a stochastic process in the next moment of time depends only on its value on the previous time step (i.e., no dependence on former "history" exists). One example of SBM is the dynamics of cooling granular gases [94]. In the standard formulation, SBM features a power-law-like dependence of the diffusivity with time, $D(t) \propto t^{\alpha-1}$ [56,57,94,116,117] (see Table I). For a "critical" exponent of this time dependence, namely, at $D(t) \propto 1/t$, SBM gives rise to ultraslow diffusion with a logarithmic growth of the MSD at long times, $\mathrm{MSD}(t) \propto \log(t/\tau)$ [95]. The exponential growth of the long-time MSD and the linear growth of the short-time TAMSD are the characteristic features of GBM [49,50] as well as of exponential SBM with $D(t) \propto e^{\kappa t}$ introduced in Ref. [118]. These SBM-type processes exhibit a linear growth of the TAMSD with the lag time.

FBM [54,55] is a very widely used stochastic process employed to describe subdiffusion in viscoelastic [119] systems such as the cyto- and nucleoplasm of diverse classes of biological cells [38,120] on various length- and time-scales (among other numerous applications [14]). FBM is a Gaussian process [30,121] with stationary increments which are persistent and antipersistent for the anomalous Hurst exponent H in the range $2 > 2H > 1$ and $0 < 2H < 1$, respectively. FBM with $2H = 1$ reduces to BM. FBM is "nearly" ergodic [66,69,74], being one of few stochastic processes with a nonlinear and H-dependent scaling exponent of the TAMSD. The property of *Gaussianity* means a Gaussian form of the distribution of position displacements of the particles, $P(x,t)$, as measured after a diffusion time t. *Stationarity* of increments of a stochastic process means their independence on the actual time moment of measurement. In addition to free-space FBM, potential-confined [122–127] and externally reset [115] FBM versions were considered as well.

D. Generalizations of diffusion models

As an even smaller subset of stochastic processes mentioned in Sec. IC, several modifications of SBM [56,94–97,118,128], FBM [74,115], and HDPs [58,59,88–91] were studied recently. A number of recent SPT data sets [38,39,129–142] indicate a motion driven by a stochastic process featuring more than a single generating mechanism. Therefore, "compound" processes with more "multifaceted" statistical characteristics [143] can be beneficial.

In particular, nonergodic processes with a nonlinear growth of the TAMSD(Δ) and with additionally tunable aging dependence on the trajectory length T (denoted as $\langle\overline{\delta^2(\Delta,T)}\rangle$) are required to rationalize some SPT data sets, namely,

$$\langle\overline{\delta^2(\Delta,T)}\rangle \propto \Delta^{\mu}/T^{1-\nu} \neq \langle x^2(\Delta)\rangle. \tag{5}$$

Such desired processes would then serve as tools to physically describe a number of "mixed" statistical properties observed in experimental SPT time series [18,19,30,39,141,142,144–150]. *Aging* here means a particular dependence of the TAMSD magnitude on the measurement time T. For multiple power-law-type subdiffusive processes the magnitude of $\langle\overline{\delta^2(\Delta,T)}\rangle$ is a decaying power-law function of T, as measured at short lag times Δ (see Table I).

The list of hybrid processes developed by us in recent years includes the processes of SBM-HDP [61], FBM-HDP [60], FBM-diffusing diffusivity [69], FBM-SBM [62], SBM-diffusing diffusivity [96,151], exponential and logarithmic HDPs [88], exponential and logarithmic SBM [118], and SBM-GBM [152] (see a short overview in Table I). Note that a hybrid diffusion process with a power-law-like time- and space-dependent diffusivity was also proposed previously in Refs. [116,153–155]. Regarding the technicalities of the

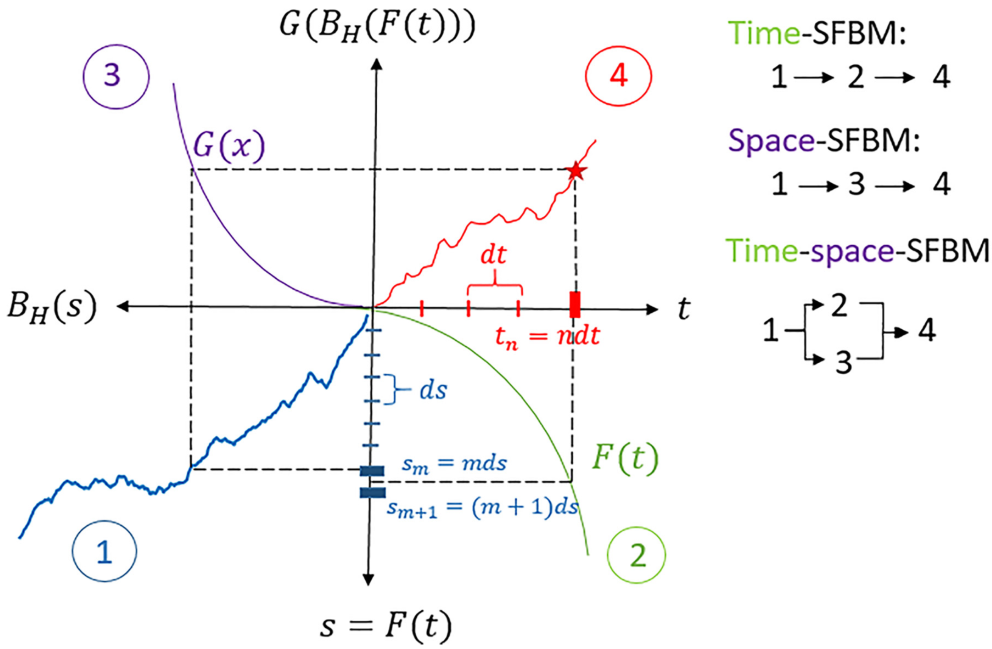

FIG. 2. Details of the simulation scheme for generating time- and space-SFBM from a parental FBM trajectory. The procedure to create SFBM from a finely simulated FBM (time-step ds) via a "projection" with rescaling functions $F(t)$ and $G(x)$ is illustrated here, see Sec. II C for details.

mathematical description and the applications of all these stochastic processes, we refer the interested reader to the original studies. Note also that an extensive collection of FBM- and SBM-related SPT experimental observations were tabulated in Ref. [62]. Recently, hybrid stochastic processes of CTRW type with a random walk on fractals [156], CTRW-FBM [18,157], and processes alternating between a Lévy walk and standard BM [158] as well as between a Lévy walk and CTRW [159,160] were proposed, in addition to other models of anomalous diffusion of mixed origin [156].

Various computational methods and statistical tests for the SPT-trajectory analysis of multiple origins (e.g., Bayesian inference, neural-network-based, power spectrum, p-variation test, and machine-learning-based approaches, etc.) have been invented in recent years [18–20,30,132,144–150,161–172] to estimate and to catalog the models of diffusion as well as to determine their parameters for a given data set (such as the MSD- and TAMSD-scaling exponents, the increment-autocorrelation functions, Mandelbrotian exponents [173], the TAMSD-aging functions, etc.). The state of the art of such analysis methods was recently assessed by the anomalous-diffusion (AnDi) challenge [18,174]. In the current investigation, we are particularly interested in these statistical quantifiers and answer the question how they change for various underlying functional forms of superimposed time and space clocks.

E. Plan of the paper

Here, we extend the arsenal of hybrid anomalous-diffusion models via presenting a generalized stochastic process of scaled fractional Brownian motion (SFBM) (see Fig. 1). The process of time-rescaled BM with nonlinear clocks in fact has some history: for power-law and logarithmic-like clock functions it was first proposed on the MSD level in Refs. [67,68]. For power-law clocks this process was named compressed or stretched BM [67] and it describes sub- or superdiffusive SBM [56,96], respectively. The process of SFBM fills the gap in understanding the principles of composition of the MSD and TAMSD scaling exponents for many of the compound stochastic processes mentioned in Sec. I D, connecting them to the features of running time and space clocks.

Time-SFBM $B_H(F(t))$ and space-SFBM $G(B_H(t))$ processes are constructed based on FBM $B_H(t)$ running with a nonlinear time clock $F(t)$ and a nonlinear space clock $G(x)$, respectively. We explicitly investigate analytically and via *in silico* experiments the properties of diffusive motion of particles by selecting different clocks giving rise to a power-law anomalous, ultraslow, and superfast diffusion described by SFBM.

The rest of this study is organized as follows. In Sec. II the processes of FBM and time SFBM are introduced. In Sec. III we describe the probability-density function (PDF), the MSD, the TAMSD, as well as provide the analysis of the nonergodic and aging behaviors of *time*-SFBM with three special cases of nonlinear time clock. In Sec. IV we introduce *space*-SFBM, computing the same characteristics for three scenarios of nonlinear space clocks. In Sec. V the properties of time-space-SFBM are examined. Finally, in Sec. VI we present the main conclusions. A number of auxiliary figures are provided in the Appendix A, while all acronyms are provided in Appendix B.

II. FBM AND TIME-SFBM

In this section, we give a brief introduction into FBM and present some results for time-SFBM that can be regarded as "merging" of FBM with SBM.

A. FBM

The process of FBM,

$$x(t) = B_H(t), \quad (6)$$

studied by Mandelbrot and van Ness [55] and in fact considered earlier by Kolmogorov [54], is a centered continuous-time Gaussian process with the two-point autocovariance function of the form

$$\langle B_H(t_1)B_H(t_2)\rangle = \frac{K_{2H}}{2}\left(t_1^{2H} + t_2^{2H} - |t_2 - t_1|^{2H}\right), \quad (7)$$

where the generalized diffusion coefficient K_{2H} has physical units

$$[K_{2H}] = \mathrm{m}^2\mathrm{s}^{-2H}, \quad (8)$$

and with the Gaussian particle-displacement form of the PDF,

$$P(x,t) = \exp\left(-\frac{x^2}{2K_{2H}t^{2H}}\right)\Big/\sqrt{2\pi K_{2H}t^{2H}}. \quad (9)$$

Here, $x_0 = 0$ is the starting position and t is diffusion time. FBM is an ergodic [14] stochastic process, with the MSD equal to the TAMSD,

$$\langle x^2(\Delta)\rangle = \langle B_H^2(\Delta)\rangle = \langle\overline{\delta^2(\Delta)}\rangle = K_{2H}\Delta^{2H}. \quad (10)$$

The mean TAMSD is generally defined as the arithmetic mean over N available statistically identical and independent particle trajectories, namely [14]

$$\langle\overline{\delta^2(\Delta)}\rangle = \frac{1}{N}\sum_{i=1}^{N}\overline{\delta_i^2(\Delta)}. \quad (11)$$

The stationarity of increments of FBM can be studied via its autocovariance function. Considering an increment [55]

$$B_H^{(\delta)}(t) = B_H(t+\delta) - B_H(t), \quad (12)$$

the autocovariance function between the increments in the intervals $[t_1, t_1+\delta]$ and $[t_2, t_2+\delta]$ is defined as

$$C^{(\delta)}(t_1,t_2) = \langle B_H^{(\delta)}(t_1)B_H^{(\delta)}(t_2)\rangle. \quad (13)$$

Using Eq. (7) we arrive at the autocovariance function of FBM that solely depends on the time difference $\Delta_{12} = |t_2 - t_1|$ (with $t_2 > t_1$), namely,

$$C^{(\delta)}(t_1,t_2) = \frac{K_{2H}}{2}\left((\Delta_{12}+\delta)^{2H} + |\Delta_{12}-\delta|^{2H} - 2\Delta_{12}^{2H}\right). \quad (14)$$

In particular, when $\Delta_{12} \gg \delta$ the autocovariance function has an approximate power-law form

$$C^{(\delta)}(t_1,t_2) \sim K_{2H}H(2H-1)\delta^2 \times \Delta_{12}^{2H-2}, \quad (15)$$

indicating that FBM has positively and negatively correlated increments for $1 > H > 1/2$ and $0 < H < 1/2$, respectively [55].

B. Time-SFBM

Time-SFBM is defined as a stochastic process of FBM running with a nonlinear time clock, i.e.,

$$x(t) = B_H(F(t)). \quad (16)$$

Here $F(t)$ is a deterministic smooth monotonic function changing over time with a non-negative derivative $f(t)$ satisfying (see also Refs. [67,68] employing the same method for clarification of its requirements)

$$F(t) = \int_0^t D_\alpha f(s)ds. \quad (17)$$

Here D_α is a coefficient ensuring that $F(t)$ always has the dimension of time, $[F] = \mathrm{s}^1$. Combining the property of FBM (7) and the definition (16) yields the two-point autocovariance function of time-SFBM as

$$\langle x(t_1)x(t_2)\rangle = \frac{K_{2H}}{2}([F(t_1)]^{2H} + [F(t_2)]^{2H} - |F(t_1) - F(t_2)|^{2H}). \quad (18)$$

When $t_1 = t_2 = t$ the MSD of time-SFBM reads

$$\langle x^2(t)\rangle = K_{2H}[F(t)]^{2H}. \quad (19)$$

Using definition (4), the mean TAMSD of time-SFBM is

$$\langle\overline{\delta^2(\Delta)}\rangle = \frac{K_{2H}}{T-\Delta}\int_0^{T-\Delta}[F(t+\Delta) - F(t)]^{2H}dt. \quad (20)$$

When $\Delta \ll T$, using the Taylor expansion $F(t+\Delta) - F(t) \approx D_\alpha f(t)\Delta$, we get the leading term

$$\langle\overline{\delta^2(\Delta)}\rangle \approx \frac{K_{2H}}{T}\left[\int_0^T [D_\alpha f(t)]^{2H}dt\right] \times \Delta^{2H}. \quad (21)$$

Obviously, the TAMSD (21) is not equivalent to the MSD (19), indicating weak ergodicity breaking as long as $F(t)$ is a nonlinear function. Notably, when $H = 1/2$ time-SFBM reduces to SBM [56,57,94,116,117] with

$$\langle\overline{\delta^2(\Delta)}\rangle = K_1F(T) \times \Delta/T. \quad (22)$$

Given the increments (12), for $x_\delta(t) = x(t+\delta) - x(t)$ of time-SFBM we have

$$x_\delta(t) = B_H(F(t+\delta)) - B_H(F(t)) \quad (23)$$

and the explicit autocovariance function can be obtained as

$$C^{(\delta)}(t_1,t_2) = \frac{K_{2H}}{2}(|F(t_1+\delta) - F(t_2)|^{2H} + |F(t_1) - F(t_2+\delta)|^{2H} - |F(t_1+\delta) - F(t_2+\delta)|^{2H} - |F(t_1) - F(t_2)|^{2H}). \quad (24)$$

This implies that, as expected, the property of stationarity is broken when FBM runs with a nonlinear clock. In particular, when $H = 1/2$ we get $C^{(\delta)}(t_1,t_2) = 0$ if the two increments in the intervals $[t_1, t_1+\delta]$ and $[t_2, t_2+\delta]$ are disjoint. This feature reveals that FBM with arbitrary nonlinear clocks has independent increments.

The PDF of time-SFBM with arbitrary nonlinear clock is—analogously to FBM expression (9)—a Gaussian function

$$P(x,t) = \exp\left(-\frac{x^2}{2K_{2H}[F(t)]^{2H}}\right)\Big/\sqrt{2\pi K_{2H}[F(t)]^{2H}}. \quad (25)$$

C. Details of computer simulations

The trajectories of SFBM are generated below from those of standard FBM through the specific transformations of time-and space-related variables. In short, several standard methods can be employed to generate FBM [176] including, e.g., the method of Hosking [177], the Choleski matrix-decomposition approach, or the method of Wood and Chan [178]. We adopt here the last one [178], used also in Refs. [69,70], due to its rapid simulation times achieved by using the discrete Fourier transformation [179].

To generate time-SFBM (16) as $x(t) = B_H(F(t))$ in Sec. III at discrete times $t_n = n \times dt$, where $dt = T/N$ is the time step and T is the measurement time, we find equivalent discrete points of $B_H(s)$ at times

$$s_m = m \times ds = F(t_n). \tag{26}$$

Here $ds < dt$ is a smaller time step to generate FBM. As the time-transformation function $F(t)$ is general, an integer m obeying (26) does not always exit. We thus find adjacent points t_m and t_{m+1} such that

$$m \times ds \leqslant F(t_n) < (m+1) \times ds \tag{27}$$

is fullfilled in order to approximate $F(t_n)$ (see the details in Fig. 2). This method is frequently employed to generate subordinated stochastic processes [180].

The discrete-time process (16) is thus approximated in two steps:

(i) We first generate FBM trajectories using the method of Wood and Chan [178]; e.g., we create $B_H(s_j)$ at discrete times and with the trajectory length $s_{\max} \geqslant F(T)$.

(ii) The values of $x(t_n)$ are equivalent to those of $B_H(s_j)$ with $s_j = \text{round}[F(t_n)/ds]$, where round$[x]$ produces a ceiling integer for x. The more rapid the variation of $F(t)$ with time is, the more detailed should the simulation grid ds for the initial FBM process be in order for the final time-SFBM process to be sufficiently accurate.

Figures 12, 15, and 18 demonstrate the consistency of the simulations and analytical results for the MSD and the mean TAMSD for time-SFBM with power-law, logarithmic, and exponential time clocks for the three relationships

$$ds = dt/2,\ ds = dt/5,\ ds = dt/10. \tag{28}$$

The last choice yields (naturally) the most accurate results.

To simulate space-SFBM defined via (48) as $y(t) = G(B_H(t))$ in Sec. IV, as the timescale does not change upon transformation $B_H(t) \to y(t)$, the discrete-time process $y(t_n)$ follows directly via finding the related point of FBM $B_H(t_m)$ at $t_m = t_n$, and then mapping the values of FBM with the specific nonlinear space transformation. The most general time-space-SFBM examined in Sec. V is simulated as a point process $z(t_n) = G(x(t_n))$ through a particular space transformation $G(x)$ and time transformation $F(t)$. This gives $x(t_n) = B_H(F(t_n))$ that yields $z(t_n) = G(B_H(F(t_n)))$. The time-transformed process $x(t_n) = B_H(F(t_n))$ is generated again by the approximate approach for time-SFBM outlined above.

III. SPECIAL CASES OF TIME-SFBM

In this section, the results for three special situations of time-SFBM for nonlinear power-law, logarithmic, and exponential time clocks are presented. We demonstrate that time-SFBM in all these situations is a nonergodic and aging stochastic process.

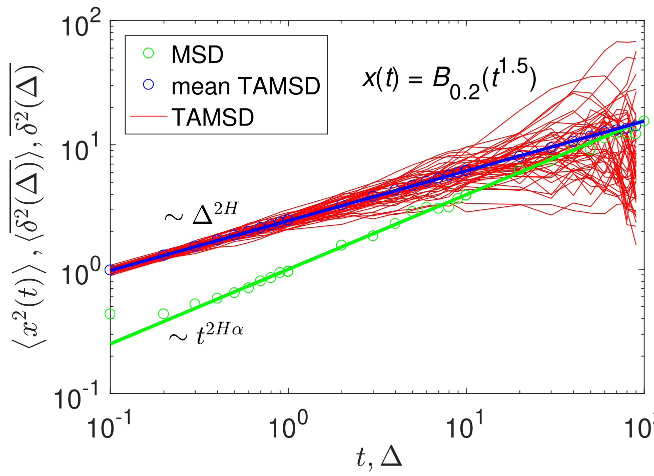

FIG. 3. Magnitude of the MSD (green circles), the spread of individual TAMSDs (thin red curves), and the mean time transformation TAMSD (blue circles) for the process of time-SFBM with time transformation (29) computed for the Hurst exponent $H = 0.2$ and the exponent $\alpha = 1.5$. Theoretical results for the MSD (thick solid green curves) and the mean TAMSD (thick solid blue curves) are given by Eqs. (31) and (32), respectively; the respective short-time scaling exponents are added in the graph for clarity. Parameters: the length of the trajectories is $T = 100$, the elementary time step in computer simulations is $dt = 0.1$, the FBM generalized diffusion coefficient is $K_{2H} = 1$ (hereafter, for all diffusion-coefficient-like quantities we do not mention their explicit units), the coefficient D_α is $D_\alpha = 1$, and the number of independent trajectories (ensemble size) is $N = 300$.

A. Anomalous diffusion with $F(t) = D_\alpha t^\alpha$

For the choice

$$F(t) = D_\alpha t^\alpha, \tag{29}$$

with $\alpha > 0$ and D_α having physical units

$$[D_\alpha] = \mathrm{s}^{1-\alpha}, \tag{30}$$

the time-SFBM describes anomalous diffusion with the MSD

$$\langle x^2(t)\rangle = K_{2H}(D_\alpha)^{2H} t^{2H\alpha}, \tag{31}$$

while the mean TAMSD (at short lag times $\Delta \ll T$) is given by

$$\langle\overline{\delta^2(\Delta)}\rangle = \frac{K_{2H}(\alpha D_\alpha)^{2H}}{2H(\alpha-1)+1} \times \frac{\Delta^{2H}}{T^{2H(1-\alpha)}}. \tag{32}$$

Both the MSD and the mean TAMSD are power-law functions of time.

The TAMSD magnitude depends on the trajectory length T and thus the current process features aging [14]. Based on the mean-TAMSD result (32), the TAMSD aging factor can be quantified for short lag times as

$$\Lambda(T) \simeq T^{2H(\alpha-1)}. \tag{33}$$

Figure 3 demonstrates the consistency of the simulation results for the MSD and the mean TAMSD for time-SFBM with the clock (29) with the analytical predictions. This agreement is found in the entire range of the lag times examined. In Fig. 13 we show the excellent agreement of the results from simulations and the theory for the Gaussian PDF of time-SFBM (29), for H and α values as in Fig. 3. Figure 14 shows the agreement of simulations and theory for the aging factor: it has a power-law dependence on T as a function of the values of H and α. Here and below, we present the dimensionless aging factor Λ.

B. Ultraslow diffusion with $F(t) = \mathcal{D}_\beta \log^\beta(t/\tau + 1)$

The process of time-SFBM describes ultraslow diffusion for the choice

$$F(t) = \mathcal{D}_\beta \log^\beta(t/\tau + 1), \tag{34}$$

with $\mathcal{D}_\beta$ having physical units $[\mathcal{D}_\beta] = \mathrm{s}^1$. We thus arrive at Sinai-type ultraslow growth of the MSD,

$$\langle x^2(t)\rangle = K_{2H}(\mathcal{D}_\beta)^{2H}[\log(t/\tau + 1)]^{2H\beta}, \tag{35}$$

where τ is a characteristic time of time variation of $F(t)$.

1. Case $0 < H < 1/2$

The mean TAMSD for this ultraslow-in-MSD diffusion at $0 < H < 1/2$ is a subdiffusive function of lag time, namely

$$\langle\overline{\delta^2(\Delta)}\rangle = \frac{K_{2H}(\beta\mathcal{D}_\beta)^{2H}\tau^{1-2H}}{2H(\beta-1)+1}\frac{\Delta^{2H}}{T}[\log(T/\tau)]^{2H(\beta-1)+1} \times M[2H(\beta-1)+1, 2H(\beta-1)+2, (1-2H)\log(T/\tau)], \tag{36}$$

where $M(x, y, z)$ is the Kummer function [181] of the first kind,

$$M(x, y, z) = \frac{\Gamma(y)}{\Gamma(x)\Gamma(y-x)}\int_0^1 e^{zu}u^{x-1}(1-u)^{y-x-1}du. \tag{37}$$

The logarithmic as well as the linear dependencies on the trajectory length T enter the aging-related prefactor in expression (36), while the scaling with the lag time is FBM-like, $\langle\overline{\delta^2(\Delta)}\rangle \propto \Delta^{2H}$. When $T \to \infty$, the mean TAMSD in this domain of H exponents becomes considerably simpler, namely

$$\langle\overline{\delta^2(\Delta)}\rangle \simeq K_{2H}(\mathcal{D}_\beta)^{2H}\frac{\log^{2H(\beta-1)}(T/\tau)}{T^{2H}}\Delta^{2H}. \tag{38}$$

The TAMSD aging factor in this case can thus be quantified for short lag times (when $\Delta = 1$ and $T \to \infty$) in terms of the measurement time T as

$$\Lambda(T) \simeq \frac{\log^{2H(\beta-1)}(T/\tau)}{T^{2H}}. \tag{39}$$

2. Case $H > 1/2$

The MSD for ultraslow diffusion at $1 > H > 1/2$ still follows expression (35), while the mean TAMSD in this case is

$$\langle\overline{\delta^2(\Delta)}\rangle = \frac{K_{2H}(\beta\mathcal{D}_\beta)^{2H}\tau^{1-2H}}{(2H-1)^{2H(\beta-1)+1}}\frac{\Delta^{2H}}{T} \times \gamma(2H(\beta-1)+1, (2H-1)\log(T/\tau)), \tag{40}$$

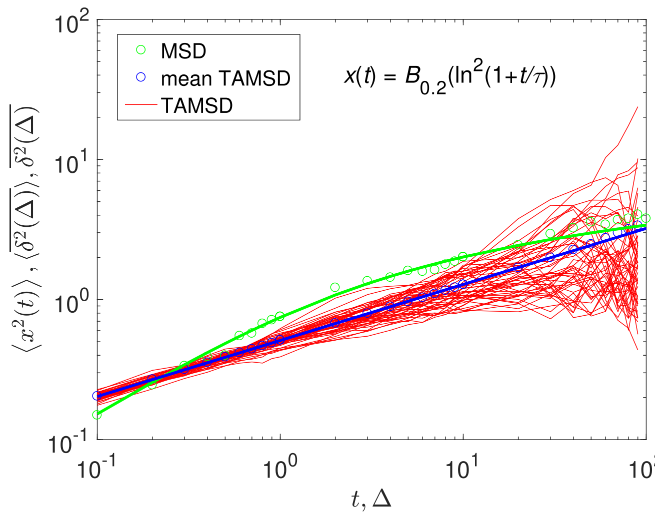

FIG. 4. MSD [Eq. (35)], TAMSDs, and mean TAMSD [Eq. (36)] for the time-SFBM with clock dependence (34) for $H = 0.2$, $\beta = 2$, $\tau = 10 \times dt$, $K_{2H} = 1$, and $\mathcal{D}_\beta = 1$. Other parameters are as in Fig. 3 (it is the case in this and all other plots of the main text and in the Appendix A, if not specified otherwise).

where $\gamma(x, y)$ is the lower incomplete Eulerian Gamma function [182]

$$\gamma(x, y) = \int_0^y u^{x-1}e^{-u}du. \tag{41}$$

When $T \to \infty$ the mean TAMSD in this case becomes

$$\langle\overline{\delta^2(\Delta)}\rangle \simeq K_{2H}(\mathcal{D}_\beta)^{2H}\tau^{1-2H}\frac{\Delta^{2H}}{T}. \tag{42}$$

This expression, again, demonstrates (in the leading order) the FBM-type growth TAMSD(Δ) $\propto \Delta^{2H}$ and the reciprocal dependence of TAMSD on the trajectory length T. The TAMSD aging factor at $\Delta/T \ll 1$ and for $H > 1/2$ is therefore

$$\Lambda(T) \simeq T^{-1}. \tag{43}$$

3. Graphical results

In Fig. 4 we observe a full consistency between the theory and simulation results for the MSD and the mean TAMSD of time-SFBM with Eq. (34), computed for $H = 0.2$ and $\beta = 2$. The MSD and the mean TAMSD agree both for short, intermediate, and long (lag) times. The stochastic process of time-SFBM running with a logarithmic time clock is evidently nonergodic. Figure 16 shows the Gaussian PDF of this process, with the analytical results fully consistent with the simulations. Figure 17 illustrates the excellent theory-vs-simulations agreement for the aging factor (39), computed for varying times T.

C. Superfast diffusion with $F(t) = \mathfrak{D}_\kappa e^{\kappa t}$

The time-SFBM gives rise to superfast diffusion when the clock function is exponential,

$$F(t) = \mathfrak{D}_\kappa e^{\kappa t}, \tag{44}$$

where κ is the reciprocal timescale of $F(t)$ variation and the coefficient $\mathfrak{D}_\kappa$ has physical dimension $[\mathfrak{D}_\kappa] = \mathrm{time}^1$. Note

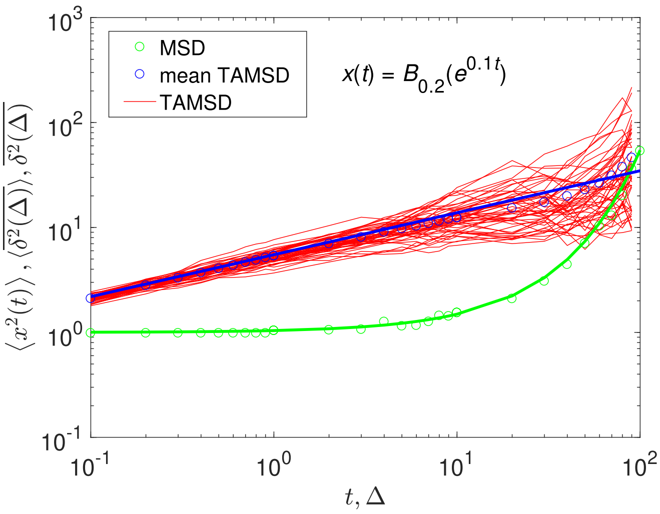

FIG. 5. MSD [Eq. (45)], TAMSDs, and mean TAMSD [Eq. (46)] for the time-SFBM with transformation (44) for $H = 0.2$, $\kappa = 0.1$, $K_{2H} = 1$, and $\mathcal{D}_\kappa = 1$.

that for each of the considered subcases of time-SFBM in subsections III A, III B, and III C we use distinct notations for the diffusion coefficients (D_α, $\mathcal{D}_\beta$, and $\mathcal{D}_\kappa$) and specify their (different) physical units. This will help to avoid confusion due to possible misinterpretation of symbols and finally yield a more systematic presentation of the results. This yields the MSD

$$\langle x^2(t)\rangle = K_{2H}(\mathcal{D}_\kappa)^{2H} e^{2H\kappa t} \tag{45}$$

and the mean TAMSD

$$\langle\overline{\delta^2(\Delta)}\rangle = \frac{K_{2H}(\mathcal{D}_\kappa)^{2H}\kappa^{2H-1}}{H}\frac{e^{2H\kappa T}-1}{T}\Delta^{2H}. \tag{46}$$

We thus find that MSD grows exponentially in time, while the TAMSD has a power-law FBM-type scaling (10) with the lag time.

Note that—similarly to Eq. (38)—the trajectory length T enters expression (46) both in a linear and logarithmic fashion, complicating the general aging behavior as compared to that known for other aging processes [14]. The mean TAMSDs of logarithmically slow MSD spreading in Sec. III B and exponentially fast MSD-related diffusion in Sec. III C have, therefore, very different functional forms. The aging function for this process can be quantified, as follows from Eq. (46), at short lag times $\Delta = 1$ for varying measurement times T as

$$\Lambda(T) \simeq \frac{e^{2H\kappa T}-1}{T}. \tag{47}$$

Figure 5 illustrates the MSD and the mean TAMSD for time-SFBM with (44) for $H = 0.2$ and $\kappa = 0.1$, in full consistency with the theoretical expectations in the whole interval of lag times. In Fig. 19 we show that the PDF of this stochastic process is Gaussian, with theoretical and simulation results being fully consistent. In Fig. 20 we present the aging factor for time-SFBM with exponential clock (44), again in full agreement with the theoretical predictions.

IV. SPECIAL CASES OF SPACE-SFBM

In this section, we present some results for space-SFBM, a process that can be considered as a hybrid of FBM and HDPs. Space-SFBM is defined through FBM running with a nonlinear "space clock,"

$$y(t) = G(B_H(t)), \tag{48}$$

where $G(x)$ is a deterministic smooth function of the space coordinate x. Some special cases of space-SFBM for power-law, logarithmic, and exponential space clocks are presented below. Similarly to time-SFBM in Sec. III, we demonstrate here that space-SFBM with all these clocks represents a non-ergodic and aging stochastic process.

For the entire consideration to be systematic, similar to time-SFBM in Sec. III with

$$[F(t)] = \text{seconds}, \tag{49}$$

for each of the subcases of space-SFBM in Secs. VI A, VI B, and VI C we use distinct (and different) notations for the diffusion coefficients, with their dimensions chosen such that the physical units of clock functions $G(x)$ always remain the same, namely

$$[G(x)] = \text{meters}. \tag{50}$$

This helps in checking physical dimensions in the resulting expressions. This can also enable experimentalists (planning to use such hybrid processes) to adjust model predictions to the measurements using these generated diffusion coefficients as additional fitting coefficients. Different notations and subscripts with the bars used for the diffusion coefficients of space-SFBM in this section—as compared to diffusivities and indices in time-SFBM in the previous section—serve the same purpose and also help us categorize different functional dependencies emerging in all the subcases.

A. Anomalous diffusion with $G(x) = \bar{D}_{\bar{\alpha}}|x|^{\bar{\alpha}}$

Space-SFBM with

$$G(x) = \bar{D}_{\bar{\alpha}}|x|^{\bar{\alpha}} \tag{51}$$

describes anomalous diffusion for $\bar{\alpha} > 0$. Here, the units of $\bar{D}_{\bar{\alpha}}$ are

$$[\bar{D}_{\bar{\alpha}}] = \text{m}^{1-\bar{\alpha}}. \tag{52}$$

The MSD of this process grows as (for the MSD, we use $\langle y^2\rangle$ for space-SFBM in Sec. IV and $\langle z^2\rangle$ for time-space-SFBM in Sec. V)

$$\langle y^2(t)\rangle = \frac{\Gamma(\bar{\alpha}+1/2)}{\sqrt{\pi}}2^{\bar{\alpha}}(K_{2H})^{\bar{\alpha}}(D_{\bar{\alpha}})^2 t^{2H\bar{\alpha}}, \tag{53}$$

while the mean TAMSD at short lag times behaves as

$$\langle\overline{\delta^2(\Delta)}\rangle = \frac{\Gamma(\bar{\alpha}+1/2)}{\sqrt{\pi}}2^{\bar{\alpha}}(K_{2H})^{\bar{\alpha}}(\bar{D}_{\bar{\alpha}})^2\frac{\Delta^{2H}}{T^{2H(1-\bar{\alpha})}}. \tag{54}$$

The PDF of space-SFBM with clock (51) is described by a non-Gaussian distribution of the form

$$P(y,t) = 2\frac{y^{1/\bar{\alpha}-1}\exp\left(-\frac{y^{2/\bar{\alpha}}}{2K_{2H}(\bar{D}_{\bar{\alpha}})^{2/\bar{\alpha}}t^{2H}}\right)}{\sqrt{2\pi\bar{\alpha}^2K_{2H}(\bar{D}_{\bar{\alpha}})^{2/\bar{\alpha}}t^{2H}}}, \tag{55}$$

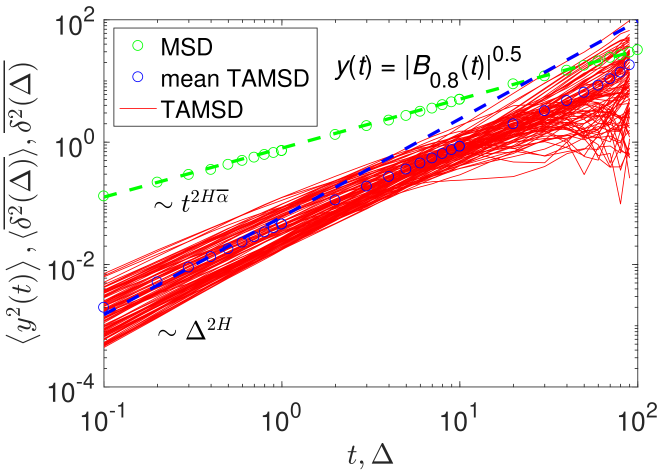

FIG. 6. MSD [Eq. (53)], TAMSDs, and mean TAMSD [Eq. (54)] for space-SFBM with clock (51) for $H = 0.8$, $\bar{\alpha} = 0.5$, $K_{2H} = 1$, and $\bar{D}_{\bar{\alpha}} = 1$.

that follows from the PDF of FBM (9) after using a HDP-like variable substitution $y(x) = \bar{D}_{\bar{\alpha}}|x|^{\bar{\alpha}} > 0$ and the probability-transformation law $P_{\rm FBM}(x)dx = P(y)dy$. The aging factor of this process is (as follows from (54))

$$\Lambda(T) \simeq T^{2H(\bar{\alpha}-1)}. \tag{56}$$

In Fig. 6 the simulations-based MSD and the mean TAMSD of space-SFBM with Eq. (51) for $H = 0.8$ and $\bar{\alpha} = 0.5$ demonstrate good agreement with theory. Note that for the MSD the agreement is quantitative at all times, while for the TAMSD at $\Delta \ll T$ the magnitude agrees well, whereas for intermediate and long lag times some deviations between the theory and respective *in silico* experiments occur. The larger the exponent $\bar{\alpha}$ is, the better the agreement between the mean TAMSD from computer simulations and the analytical predictions become (results not shown). The PDF of space-SFBM with transformation (51) is non-Gaussian (see Fig. 21), with perfect agreement of theory and simulations. In Fig. 22 the aging factor—in its variation with T—is presented.

B. Ultraslow diffusion with $G(x) = \bar{\mathcal{D}}_{\bar{\beta}} \log^{\bar{\beta}}(|x|/x_0 + 1)$

Space-SFBM with

$$G(x) = \bar{\mathcal{D}}_{\bar{\beta}} \log^{\bar{\beta}}(|x|/x_0 + 1) \tag{57}$$

describes ultraslow diffusion, with $\bar{\beta} > 0$. With units

$$[\bar{\mathcal{D}}_{\bar{\beta}}] = \mathrm{m}^1, \tag{58}$$

the MSD describing the simulation data grows as

$$\langle y^2(t)\rangle \approx \bar{\mathcal{D}}_{\bar{\beta}}^2 \log^{2\bar{\beta}}\left(\sqrt{2K_{2H}t^{2H}}/x_0 + 1\right). \tag{59}$$

The PDF of space-SFBM with (57) has—for large particle displacements and at long times—the non-Gaussian form

$$P(y,t) = 2\frac{(y/\bar{\mathcal{D}}_{\bar{\beta}})^{1/\bar{\beta}-1} e^{(y/\bar{\mathcal{D}}_{\bar{\beta}})^{1/\bar{\beta}}} \exp\left[-\frac{\left(e^{(y/\bar{\mathcal{D}}_{\bar{\beta}})^{1/\bar{\beta}}}-1\right)^2}{2K_{2H}t^{2H}/x_0^2}\right]}{\bar{\mathcal{D}}_{\bar{\beta}}\sqrt{2\pi\bar{\beta}^2 K_{2H}t^{2H}/x_0^2}}. \tag{60}$$

To derive MSD (59), as in Sec. IV A, we can use the PDF of FBM (9) and transform the variables $x = q\sqrt{2K_{2H}t^{2H}}$ that for $\langle y^2(t)\rangle = 2\int_0^\infty G^2(x)P_{\rm FBM}(x,t)dx$ yield

$$\langle y^2(t)\rangle = \frac{2\bar{\mathcal{D}}_{\bar{\beta}}^2}{\sqrt{\pi}}\int_0^\infty \log^{2\bar{\beta}}\left(\frac{\sqrt{2K_{2H}t^{2H}}q}{x_0}+1\right)e^{-q^2}dq. \tag{61}$$

At long times, to the same level of approximation as in Eqs. (59) and (60), this can be written in terms of a polynomial expansion (with $n = 2\bar{\beta}$)

$$\begin{aligned}\langle y^2(t)\rangle &\approx \frac{2\bar{\mathcal{D}}_{\bar{\beta}}^2}{\sqrt{\pi}}\int_0^\infty\left(\log q + \log\frac{\sqrt{2K_{2H}t^{2H}}}{x_0}\right)^{2\bar{\beta}} e^{-q^2}dq\\ &\approx \frac{2\bar{\mathcal{D}}_{\bar{\beta}}^2}{\sqrt{\pi}}\sum_{k=0}^{n}\binom{n}{k}\left[\log\frac{\sqrt{2K_{2H}t^{2H}}}{x_0}\right]^{n-k}\\ &\quad\times\int_0^\infty(\log q)^k e^{-q^2}dq.\end{aligned} \tag{62}$$

Here $\binom{n}{k} = \frac{n!}{k!(n-k)!}$ is the binomial coefficient. Due to the exponential decay, the integrals over q converge for all k values to $C_k = \int_0^\infty(\log q)^k e^{-q^2}dq$ (for $k = 0$, e.g., we get $C_0 = \sqrt{\pi}/2$). The leading term of Eq. (62) obtained at $k = 0$ gives the MSD expression (59); for small values of $\bar{\beta}$ this is the only term in the sum (62).

1. *Case* $0 < H < 1/2$

The mean TAMSD of space-SFBM at $0 < H < 1/2$ for $T/\Delta \to \infty$ is

$$\langle\overline{\delta^2(\Delta)}\rangle \approx \bar{\mathcal{D}}_{\bar{\beta}}^2\frac{\log^{2H(2\bar{\beta}-2)}\left[\left(2K_{2H}T^{2H}/x_0^2\right)^{1/(2H)}\right]}{T^{2H}}\Delta^{2H}, \tag{63}$$

with the aging function (given by its prefactor) as

$$\Lambda(T) \simeq \frac{\log^{2H(2\bar{\beta}-2)}\left[\left(2K_{2H}T^{2H}/x_0^2\right)^{1/(2H)}\right]}{T^{2H}}. \tag{64}$$

2. *Case* $H > 1/2$

The MSD for ultraslow diffusion for $H \geqslant 1/2$ still follows expression (59), while the mean TAMSD for $T/\Delta \gg \infty$ becomes

$$\langle\overline{\delta^2(\Delta)}\rangle \approx \bar{\mathcal{D}}_{\bar{\beta}}^2\left(2K_{2H}/x_0^2\right)^{1-1/(2H)}\frac{\Delta^{2H}}{T}. \tag{65}$$

The aging factor at $\Delta = 1$ for $H \geqslant 1/2$ is thus

$$\Lambda(T) \simeq (1/T). \tag{66}$$

3. *Graphical results*

The simulated MSD and the mean TAMSD presented in Fig. 7 for space-SFBM with Eq. (57) at $H = 0.8$ and $\bar{\beta} = 2$ agree nicely with the theory. The PDF of this process shown in Fig. 23 is non-Gaussian, with a similar consistency of theoretical and simulation results. The good consistency is also found for the aging factor in Fig. 24, as a function of varying observation time T.

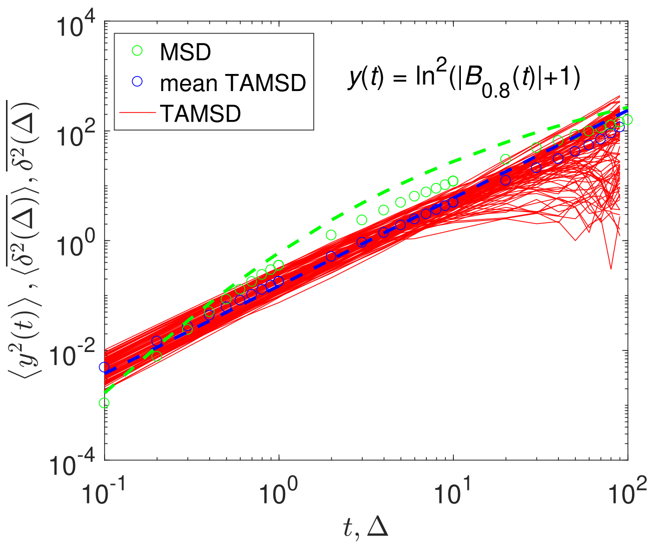

FIG. 7. MSD [Eq. (59)], TAMSDs, and mean TAMSD [Eq. (65)] for space-SFBM with clock (57) for $H = 0.8$, $\bar{\beta} = 2$, $x_0 = 1$, $K_{2H} = 1$, and $\bar{\mathcal{D}}_{\bar{\beta}} = 1$.

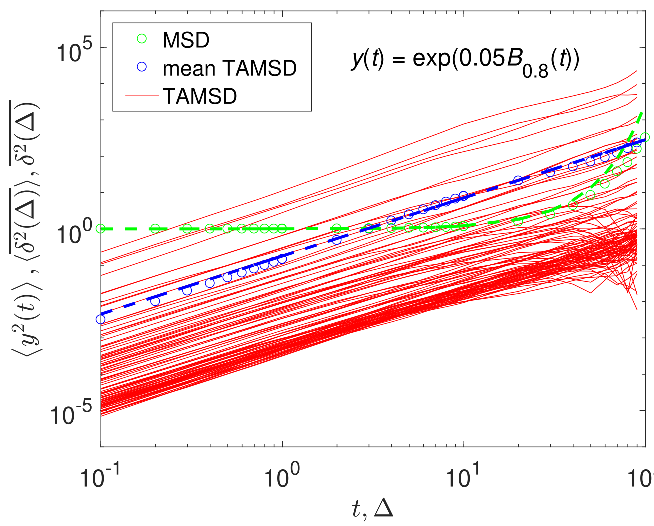

FIG. 8. MSD [Eq. (68)], TAMSDs, and mean TAMSD [Eq. (70)] for the space SFBM with (67) for $H = 0.8$, $\bar{\kappa} = 0.05$, $K_{2H} = 1$, and $\bar{\mathcal{D}}_{\bar{\kappa}} = 1$.

C. Superfast diffusion with $G(x) = \bar{\mathcal{D}}_{\bar{\kappa}} e^{\bar{\kappa}x}$

The process of space-SFBM describes superfast diffusion when

$$G(x) = \bar{\mathcal{D}}_{\bar{\kappa}} e^{\bar{\kappa}x}, \tag{67}$$

where $\bar{\kappa} > 0$ is the reciprocal length scale of $G(x)$ variation (with $[\bar{\kappa}]$=1/m and $[\bar{\mathcal{D}}_{\bar{\kappa}}] = \mathrm{m}^1$), with the MSD

$$\langle y^2(t)\rangle = \bar{\mathcal{D}}_{\bar{\kappa}}^2 \exp(2\bar{\kappa}^2 K_{2H} t^{2H}). \tag{68}$$

The PDF of space-SFBM with clock (67) is expectedly not a Gaussian, but rather a modified log-normal distribution

$$P(y,t) = \exp\left(-\frac{[\log(y/\bar{\mathcal{D}}_{\bar{\kappa}})]^2}{2K_{2H}\bar{\kappa}^2 t^{2H}}\right)\Big/\sqrt{2\pi y^2 K_{2H}\bar{\kappa}^2 t^{2H}}. \tag{69}$$

The mean TAMSD for this superfast MSD diffusion for $\Delta/T \ll 1$ is

$$\langle\overline{\delta^2(\Delta)}\rangle = \bar{\mathcal{D}}_{\bar{\kappa}}^2 \frac{e^{2K_{2H}\bar{\kappa}^2 T^{2H}}}{T^{2H}} \Delta^{2H}, \tag{70}$$

whereas the aging factor is

$$\Lambda(T) \simeq \frac{e^{2K_{2H}\bar{\kappa}^2 T^{2H}}}{T^{2H}}. \tag{71}$$

In Fig. 8 the results for the MSD and the mean TAMSD for space-SFBM with (67) for $H = 0.8$ and $\bar{\kappa} = 0.05$ are illustrated. In Fig. 25 the log-normal PDF of this process is shown, also revealing a quantitative agreement of theory and simulations. In Fig. 26 the results for the aging factor (71) are presented.

V. TIME-SPACE-SFBM

A. General concepts

Here, we present some results for the process of time-space-SFBM, which generalizes FBM, SBM, and HDPs (see below). Time-space-SFBM is effectively FBM running with a nonlinear space- and time-clock

$$z(t) = G(B_H(F(t))), \tag{72}$$

where $F(t)$ and $G(x)$ are smooth functions. Below, to stay concise, we present the results for time-space-SFBM *only* for a power-law space clock

$$G(x) = \bar{D}_{\bar{\alpha}}|x|^{\bar{\alpha}} \tag{73}$$

as per Eq. (51) used in the case of space-SFBM in Sec. IV and for the same three cases of the time-clock $F(t)$ used for time-SFBM in Sec. III. Analogously to time- and space-SFBM considered in Secs. III and IV, correspondingly, we demonstrate below that time-space-SFBM with all these choices of clocks is nonergodic and aging.

Combining the properties of time-SFBM [Eq. (19)] and space-SFBM [Eq. (53)], the PDF of time-space-SFBM is generally non-Gaussian,

$$P(z,t) = 2\frac{z^{1/\bar{\alpha}-1}\exp\left(-\left(\frac{z^2}{(2K_{2H})^{\bar{\alpha}}(\bar{D}_{\bar{\alpha}})^2[F(t)]^{2H\bar{\alpha}}}\right)^{1/\bar{\alpha}}\right)}{\sqrt{2\pi\bar{\alpha}^2[(K_{2H})^{\bar{\alpha}}(\bar{D}_{\bar{\alpha}})^2[F(t)]^{2H\bar{\alpha}}]^{1/\bar{\alpha}}}}, \tag{74}$$

and its MSD—with the chosen coefficients for fractional Gaussian noise, as well as of the space and time dependencies of the diffusion coefficient—reads

$$\langle z^2(t)\rangle = \frac{\Gamma(\bar{\alpha}+1/2)}{\sqrt{\pi}} 2^{\bar{\alpha}}(K_{2H})^{\bar{\alpha}}(\bar{D}_{\bar{\alpha}})^2[F(t)]^{2H\bar{\alpha}}. \tag{75}$$

The factor 2 in Eq. (74) (and in the PDF relations below) stems from the definitions (72) and (51) reducing the domain of definition of this process to the $z > 0$ region. This fact finds its reflection also in the PDF plots presented in the Appendix A, all showing only one "wing" of the particle-position distribution functions.

B. Limiting behaviors of space-time-SFBM: HDP, SBM-HDP, SBM, FBM-HDP, and FBM with diffusing diffusivity

Naturally, the most general space-time-SFBM process reduces to a number of previously investigated anomalous stochastic processes for the following choices of exponents of the time- and space-transformation functions.

(i) For the choice $H = 1/2$, with $G(x) = \bar{D}_{\bar{\alpha}}|x|^{\bar{\alpha}}$, and with $F(t) = D_1 t^1$ we arrive at the HDP with (after setting $\bar{\alpha} = p$ and redefining the coefficients as $\bar{D}_{\bar{\alpha}}^{2/\bar{\alpha}} = \frac{(2/p)^2 D_{0,\text{HDP}}}{2K_1 D_1}$ to get the form of Eqs. (2) and (3) in Ref. [58]) the PDF

$$P(z,t) = 2\frac{z^{1/p-1}\exp\left(-\frac{z^{2/p}}{(2/p)^2 D_{0,\text{HDP}}t}\right)}{\sqrt{4\pi D_{0,\text{HDP}}t}}, \tag{76}$$

and the MSD

$$\langle z^2(t)\rangle = \int_0^\infty z^2 P(z,t)dz = \frac{\Gamma(p+1/2)}{\sqrt{\pi}}\left(\frac{2}{p}\right)^{2p}(D_{0,\text{HDP}})^p t^p. \tag{77}$$

(ii) For $H = 1/2$, $G(x) = \bar{D}_{\bar{\alpha}}|x|^{\bar{\alpha}}$, and $F(t) = D_\alpha t^\alpha$ the process of space-time-SFBM reduces to SBM-HDP with (setting $\bar{\alpha} = p$ and redefining the exponent $\alpha = \beta_{\text{SBM-HDP}} + 1$ and the coefficients $\bar{D}_{\bar{\alpha}}^{2/\bar{\alpha}} = \frac{(2/p)^2 D_{0,\text{SBM-HDP}}}{2K_1 D_\alpha}$ to get Eqs. (18) and (20) in Ref. [61]) the general PDF (74) that turns into

$$P(z,t) = 2\frac{z^{1/p-1}\exp\left(-\frac{z^{2/p}}{(2/p)^2 D_{0,\text{SBM-HDP}}t^\alpha}\right)}{\sqrt{4\pi D_{0,\text{SBM-HDP}}t^\alpha}}, \tag{78}$$

and the MSD

$$\langle z^2(t)\rangle = \frac{\Gamma(p+1/2)}{\sqrt{\pi}}\left(\frac{2}{p}\right)^{2p}(D_{0,\text{SBM-HDP}})^p t^{\alpha\times p}. \tag{79}$$

(iii) For $H = 1/2$, $\bar{\alpha} = 1$, and $F(t) = D_\alpha t^\alpha$ time-space-SFBM with Eqs. (74) and (75) yields (with the redefinition $\mathcal{K}_{\alpha,\text{SBM}} = K_1\bar{D}_1^2 D_\alpha$) the process of SBM featuring the PDF

$$P(z,t) = 2\exp\left(-\frac{z^2}{2\mathcal{K}_{\alpha,\text{SBM}}t^\alpha}\right)/\sqrt{2\pi\mathcal{K}_{\alpha,\text{SBM}}t^\alpha} \tag{80}$$

and the MSD

$$\langle z^2(t)\rangle = \mathcal{K}_{\alpha,\text{SBM}}t^\alpha. \tag{81}$$

(iv) For arbitrary H values, $G(x) = \bar{D}_{\bar{\alpha}}|x|^{\bar{\alpha}}$, and $F(t) = D_1 t^1$ space-time-SFBM turns (with the substitution $\bar{\alpha} = p$ and $\bar{D}_{\bar{\alpha}}^{2/\bar{\alpha}} = \frac{(2/p)^2 D_{0,\text{FBM-HDP}}}{2K_{2H}D_1^{2H}}$ to get the equivalence with Eqs. (38) and (40) in Ref. [60]) into the process of FBM-HDP with the PDF

$$P(z,t) = 2\frac{z^{1/p-1}\exp\left(-\frac{z^{2/p}}{(2/p)^2 D_{0,\text{FBM-HDP}}t^{2H}}\right)}{\sqrt{4\pi D_{0,\text{FBM-HDP}}t^{2H}}}, \tag{82}$$

and the MSD

$$\langle z^2(t)\rangle = \frac{\Gamma(p+1/2)}{\sqrt{\pi}}\left(\frac{2}{p}\right)^{2p}(D_{0,\text{FBM-HDP}})^p t^{p\times 2H}. \tag{83}$$

In turn, FBM-HDP turns into HDP at $H = 1/2$ and into FBM at $p = 1$. Lastly, we note that—similarly to the limiting behaviors of space-time-SFBM—the process of space-SFBM considered in Sec. IV with $H = 1/2$ turns into HDP (with variable $\bar{\alpha}$) and with $\bar{\alpha} = 1$ it becomes FBM (with variable $2H$).

(v) Finally, stochastic processes of BM with diffusing diffusivity and FBM with diffusing diffusivity with, respectively, normal MSD$(t) \propto t$ [82] and non-Fickian MSD$(t) \propto t^{2H}$ [69,70] can in some aspects be modeled by time-space-SFBM. Note that the PDFs of many diffusing-diffusivity models feature a crossover from a Laplacian at short times to a Gaussian at long times. This can be mimicked by time-space-SFBM with different model parameters in the current consideration. For instance, for time-space-SFBM (72) with functions $F(t)$ (29) and $G(x)$ (51) with $\alpha = 1/2$ and $\bar{\alpha} = 2$ we arrive at the Laplacian PDF

$$P(z,t) = \frac{z^{-1/2}\exp\left(-\frac{z}{2K_{2H}\bar{D}_2 D_{1/2}^{2H}t^H}\right)}{\sqrt{2\pi K_{2H}\bar{D}_2 D_{1/2}^{2H}t^H}}, \tag{84}$$

and the MSD

$$\langle x^2(t)\rangle = 3K_{2H}^2\bar{D}_2^2 D_{1/2}^{4H}\times t^H. \tag{85}$$

In contrast, for $\alpha = 1$ and $\bar{\alpha} = 1$ the Gaussian distribution

$$P(z,t) = 2\frac{\exp\left(-\frac{z^2}{2K_{2H}\bar{D}_1^2 D_1^{2H}t^{2H}}\right)}{\sqrt{2\pi K_{2H}\bar{D}_1^2 D_1^{2H}t^{2H}}} \tag{86}$$

and the MSD

$$\langle x^2(t)\rangle = K_{2H}\bar{D}_1^2 D_1^{2H}\times t^{2H} \tag{87}$$

are obtained. For comparison, for the FBM-diffusing-diffusivity model in the entire range of times in the domain of the Hurst exponent $1/2 < H < 1$, the MSD is (see Eq. (20) in Ref. [69])

$$\langle z^2(t)\rangle \approx D_{2H,\text{FBM-DD}}\times t^{2H}. \tag{88}$$

Here, the diffusion coefficient is expressed via the strength of the noise σ causing diffusivity fluctuations and the correlation time of FBM-(diffusing diffusivity) τ as follows $D_{2H,\text{FBM-DD}} = (2\pi)^{-1}\widetilde{D_{2H}}\sigma^2\tau$.

Note also that introduction of distinct diffusion coefficients for the parental processes enables a systematic consideration and allows us to change the contribution of the space, time, and noise effects into the final process separately. This, together with the unit definitions (8), (52), (30) and with a redefinition of the diffusivities (as conducted above), also helps in checking the physical dimensions at each step of the calculation.

C. Anomalous diffusion with $F(t) = D_\alpha t^\alpha$

For time-space-SFBM with clocks (51) and (29) the MSD is given by

$$\langle z^2(t)\rangle = \frac{\Gamma(\bar{\alpha}+1/2)}{\sqrt{\pi}}2^{\bar{\alpha}}(K_{2H})^{\bar{\alpha}}(\bar{D}_{\bar{\alpha}})^2(D_\alpha)^{2H\bar{\alpha}}t^{2H\bar{\alpha}\alpha}, \tag{89}$$

the mean TAMSD follows the dependence

$$\langle\overline{\delta^2(\Delta)}\rangle = \frac{\Gamma(\bar{\alpha}+1/2)}{\sqrt{\pi}}2^{\bar{\alpha}}(K_{2H})^{\bar{\alpha}}(\bar{D}_{\bar{\alpha}})^2(D_\alpha)^{2H\bar{\alpha}}\frac{\Delta^{2H}}{T^{2H(1-\bar{\alpha}\alpha)}}, \tag{90}$$

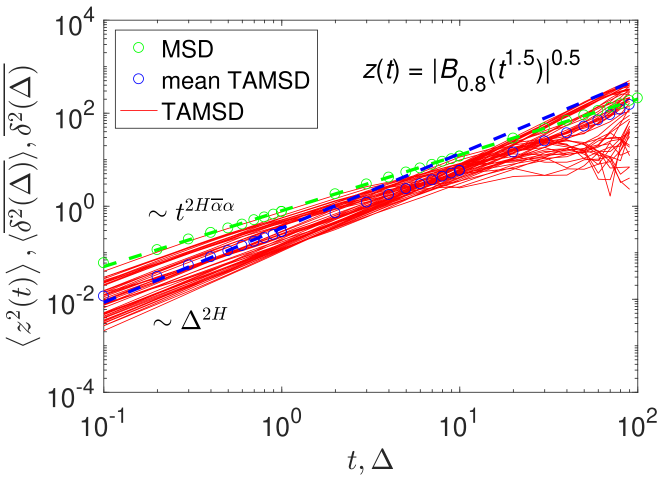

FIG. 9. MSD [Eq. (89)], TAMSDs, and mean TAMSD [Eq. (90)] for time-space-SFBM with clocks (29) and (51) for $H = 0.8$, $K_{2H} = 1$, $\alpha = 1.5$ (time clock), $\bar{\alpha} = 0.5$ (space clock), $\bar{D}_{\bar{\alpha}} = 1$, and $D_\alpha = 1$.

and the aging factor at short lag times has the form

$$\Lambda(T) \simeq T^{2H(\bar{\alpha}\alpha-1)}. \tag{91}$$

The MSD, the TAMSDs, and the mean TAMSD of time-space-SFBM with (29) and (51) are illustrated in Fig. 9, revealing a nice consistency between the theoretical predictions and simulations. The PDF of this process is shown in Fig. 27 for the same values of the exponents and model parameters. The aging factor is presented for varying observation times T in Fig. 28.

D. Ultraslow diffusion with $F(t) = \mathcal{D}_\beta[\log(t/\tau + 1)]^\beta$

Time-space-SFBM represents ultraslow diffusion with clocks (51) and (34) yielding the MSD

$$\langle z^2(t)\rangle = \frac{\Gamma(\bar{\alpha}+1/2)}{\sqrt{\pi}} 2^{\bar{\alpha}}(K_{2H})^{\bar{\alpha}}(\bar{D}_{\bar{\alpha}})^2(\mathcal{D}_\beta)^{2H\bar{\alpha}} \times [\log(t/\tau+1)]^{2H\bar{\alpha}\beta}. \tag{92}$$

1. Case $0 < H < 1/2$

The mean TAMSD at $0 < H < 1/2$ is

$$\langle\overline{\delta^2(\Delta)}\rangle = \frac{\Gamma(\bar{\alpha}+1/2)}{\sqrt{\pi}} 2^{\bar{\alpha}} \frac{(K_{2H})^{\bar{\alpha}}(\bar{D}_{\bar{\alpha}})^2(\mathcal{D}_\beta)^{2H\bar{\alpha}}}{\tau^{2H-1}} \times \frac{\Delta^{2H}}{T}\left[\log\left(\frac{T}{\tau}\right)\right]^{2H(\bar{\alpha}\beta-1)+1} \times M[2H(\bar{\alpha}\beta-1)+1, 2H(\bar{\alpha}\beta-1)+2, (1-2H)\log(T/\tau)], \tag{93}$$

that for long trajectories and short lag times turns into

$$\langle\overline{\delta^2(\Delta)}\rangle \simeq (K_{2H})^{\bar{\alpha}}(\bar{D}_{\bar{\alpha}})^2(\mathcal{D}_\beta)^{2H\bar{\alpha}} \times \frac{\log^{2H(\bar{\alpha}\beta-1)}(T/\tau)}{T^{2H}}\Delta^{2H}. \tag{94}$$

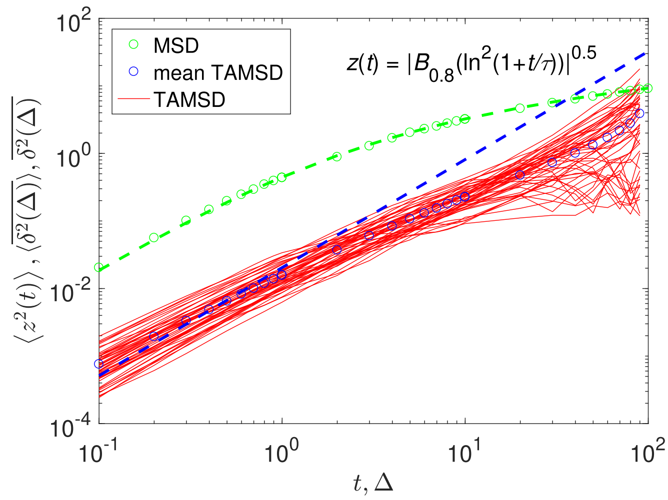

FIG. 10. MSD [Eq. (92)], TAMSDs, and mean TAMSD [Eq. (96)] of time-space-SFBM with clocks (51) and (34) for $H = 0.8$, $K_{2H} = 1$, $\beta = 2$, $\bar{\alpha} = 0.5$, $\tau = 10 \times dt$, $\bar{D}_{\bar{\alpha}} = 1$, and $\mathcal{D}_\beta = 1$.

The aging factor of this process at $H < 1/2$ is thus

$$\Lambda(T) \simeq \frac{\log^{2H(\bar{\alpha}\beta-1)}(T/\tau)}{T^{2H}}. \tag{95}$$

2. Case $H > 1/2$

The mean TAMSD of space-time-SFBM at $H > 1/2$ is

$$\langle\overline{\delta^2(\Delta)}\rangle = \frac{\Gamma(\bar{\alpha}+1/2)}{\sqrt{\pi}} 2^{\bar{\alpha}}(K_{2H})^{\bar{\alpha}}(\bar{D}_{\bar{\alpha}})^2(\mathcal{D}_\beta)^{2H\bar{\alpha}} \times \tau^{1-2H}(1/T)\Delta^{2H} \times \gamma[2H(\bar{\alpha}\beta-1)+1, (2H-1)\log(T/\tau)], \tag{96}$$

where the function γ is given by Eq. (41). At $T \to \infty$ this mean TAMSD turns into

$$\langle\overline{\delta^2(\Delta)}\rangle \simeq (K_{2H})^{\bar{\alpha}}(\bar{D}_{\bar{\alpha}})^2(\mathcal{D}_\beta)^{2H\bar{\alpha}} \times \tau^{1-2H}(1/T)\Delta^{2H}. \tag{97}$$

The aging effect for $H > 1/2$ is (cf. Sec. III B)

$$\Lambda(T) \simeq (1/T). \tag{98}$$

3. Graphical results

Figure 10 summarizes the results for the MSD, the spread of the TAMSDs, and the mean TAMSD for time-space-SFBM with space- and time-transformations (51) and (34) for $H = 0.8$, $\bar{\alpha} = 0.5$, and $\beta = 2$. Figure 29 illustrates the non-Gaussian PDF of this process, with full consistency of the theory and simulations. Figure 30 portrays the results for the aging factor.

E. Superfast diffusion with $F(t) = \mathfrak{D}_\kappa e^{\kappa t}$

Time-space-SFBM with clocks (51) and (44), with $1/\kappa$ being a characteristic timescale, has the exponentially fast

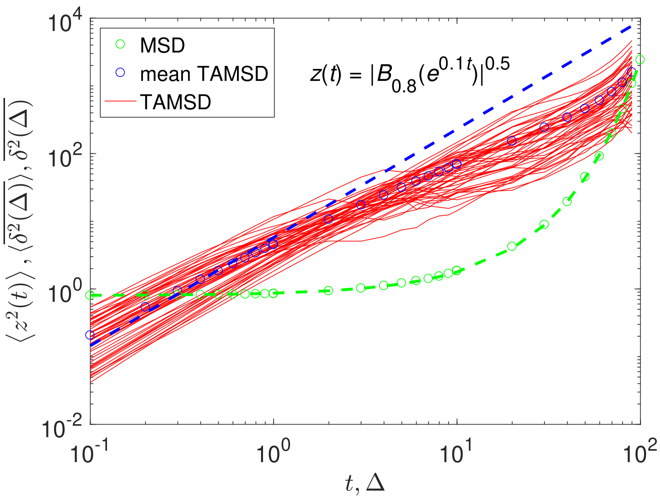

FIG. 11. MSD [Eq. (99)], TAMSDs, and mean TAMSD [Eq. (100)] for time-space-SFBM with dependencies (51) and (44) for $H = 0.8$, $K_{2H} = 1$, $\kappa = 0.1$, $\bar{\alpha} = 0.5$, $\bar{D}_{\bar{\alpha}} = 1$, and $\mathfrak{D}_\kappa = 1$.

growth of the MSD,

$$\langle z^2(t)\rangle = \frac{\Gamma(\bar{\alpha}+1/2)}{\sqrt{\pi}} 2^{\bar{\alpha}} (K_{2H})^{\bar{\alpha}} (\bar{D}_{\bar{\alpha}})^2 (\mathfrak{D}_\kappa)^{2H\bar{\alpha}} e^{2H\bar{\alpha}\kappa t}, \quad (99)$$

and the power-law evolution of the mean TAMSD,

$$\langle\overline{\delta^2(\Delta)}\rangle = \frac{\Gamma(\bar{\alpha}+1/2)}{\sqrt{\pi}} 2^{\bar{\alpha}} \frac{(K_{2H})^{\bar{\alpha}} (\bar{D}_{\bar{\alpha}})^2 (\mathfrak{D}_\kappa)^{2H\bar{\alpha}}}{\kappa^{1-2H}} \times (e^{2H\bar{\alpha}\kappa T}/T)\Delta^{2H}. \quad (100)$$

The aging factor can therefore be expressed as

$$\Lambda(T) \simeq (e^{2H\bar{\alpha}\kappa T}/T). \quad (101)$$

In Fig. 11 we illustrate the results for the MSD, the TAMSDs, and the mean TAMSD of time-space-SFBM with (51) and (44). Similarly to the observations for the MSD and the TAMSD presented in Secs. IV A, V C, and V D, the results for the mean TAMSD in Fig. 11 are in close agreement with the simulations at short lag times only, while the MSD agrees in the entire range of times; the mean TAMSD at intermediate and long lag times deviates somewhat from the theoretical predictions. Statistically most meaningful is the region of short lag times, however [14]. In Fig. 31 we show the simulated non-Gaussian PDF of this process, fully corroborating the theoretical results. Figure 32 demonstrates the behavior of the aging factor.

VI. DISCUSSION AND CONCLUSIONS

A. Main results

This paper extends the arsenal of "hybrid" models of anomalous diffusion via presenting a compound stochastic process of SFBM with nonlinear time- and space-related clocks. The diffusion process of time-SFBM is anomalous, Gaussian, nonergodic, and aging. The process of space-SFBM is anomalous, non-Gaussian, nonergodic, and aging. Therefore, the combined process of time-space-SFBM is anomalous, non-Gaussian, nonergodic, and aging. The multifacetedness of all possible situations and functional forms of the MSD, the TAMSD, and the TAMSD-aging dependencies are summarized in Table II (see also Table I to compare these scaling relations to those for other pure and hybrid diffusion processes).

Time- and space-SFBM processes provide a general and versatile framework for generating anomalous diffusion, offering a great flexibility to describe a wide spectrum of possible mechanisms, as observed in SPT studies. Generalizations of a nonlinear-clock approach to processes other than FBM are possible. This underlines the significance of the current theoretical SFBM development: as shown in Sec. V B, SFBM includes a multitude of previously studied stochastic processes as special cases. From the application viewpoint, the spectrum of physical systems and observations where the proposed processes of time- and space-SFBM are applicable include all physical systems describable by parental processes (see Secs. I C and I D) and goes well beyond these. With an input from a given system helping to infer the transformation functions $F(t)$ and $G(x)$, SFBM enables to design the best suited stochastic process to describe a given SPT data set.

Time-space-SFBM is a general process describing power-law anomalous, ultraslow, and superfast diffusion. A variability of the scaling exponents of the MSD and the mean TAMSD and their tunability via varying the clock parameters is not only the strength and an essential distinction of SFBM from the state-of-the-art approaches, but it also fits demands of the SPT data [164] description. The assessment procedure of the best-suited underlying diffusion process can thus be conducted more accurately. The "pure" processes are often too idealistic in terms of their initial basic postulates and have an insufficient number of tunable parameters to properly reflect the richness of a physical reality.

Based on the statistical features detected in a given data set to be studied—including the scaling exponents in expression (5), a distinct combination of the properties of nonergodicity, non-Fickianity, non-Gaussianity, aging, etc.—a decision should be taken whether a time-, space-, or time-space-SFBM is the most appropriate process. For this, possible combinations of the MSD and TAMSD exponents, TAMSD-aging functional forms, as well as of the PDF forms derived for each of these processes (as listed in Table II) should be compared to those from the experimental data. As Table II manifests, in contrast to a universal $\propto\Delta^{2H}$ scaling of the mean TAMSD, the exponents of the MSD, the space dependence of the PDFs, and the form of the TAMSD aging functions are highly variable for the chosen realizations of clock transformations in time-, space-, and time-space-SFBM. For instance, only time-SFBM is a Gaussian process, as Table I indicates. This offers a broad spectrum of possibilities for the SPT experimentalists to find a suitable SFBM to describe a given data set.

B. Other models and applications of SFBM

Let us now discuss and acknowledge other models and alternative approaches implementing the concepts similar to nonlinear clocks. Time-SBM running with a nonlinear clock—so-called compressed and stretched BM—was first constructed with independent nonstationary increments and with an *a priori* MSD in Ref. [67]. Later, based on it, time-SFBM was proposed and extensively studied on the MSD

TABLE II. Summarized functional forms of the MSD, the TAMSD, and the TAMSD-aging dependencies for time-SFBM, space-SFBM, time-space-SFBM, as well as some experimental SPT data sets as potential applications.

Processes ↓ Properties →	$\langle x^2(t)\rangle$	$\langle\overline{\delta^2(\Delta)}\rangle$	$\langle\overline{\delta^2(\Delta=1,T)}\rangle$
Time-SFBM			
$F(t)=D_\alpha t^\alpha$	$\propto t^{2H\alpha}$, Eq. (31)	$\propto\Delta^{2H}$, Eq. (32)	$\propto T^{2H(\alpha-1)}$, Eq. (33)
$F(t)=\mathcal{D}_\beta\log^\beta(t/\tau+1)$			
$0<H<1/2$	$\propto\log^{2H\beta}(t/\tau)$, Eq. (35)	$\propto\Delta^{2H}$, Eq. (38)	$\propto\frac{\log^{2H(\beta-1)}(T)}{T^{2H}}$, Eq. (39)
$H>1/2$	$\propto\log^{2H\beta}(t/\tau)$, Eq. (35)	$\propto\Delta^{2H}$, Eq. (42)	$\propto T^{-1}$, Eq. (43)
$F(t)=\mathfrak{D}_\kappa e^{\kappa t}$	$\propto e^{2H\kappa t}$, Eq. (45)	$\propto\Delta^{2H}$, Eq. (46)	$\propto\frac{e^{2H\kappa T}-1}{T}$, Eq. (47)
Space-SFBM			
$G(x)=\bar{D}_{\bar{\alpha}}\lvert x\rvert^{\bar{\alpha}}$	$\propto t^{2H\bar{\alpha}}$, Eq. (53)	$\propto\Delta^{2H}$, Eq. (54)	$\propto T^{2H(\bar{\alpha}-1)}$, Eq. (56)
$G(x)=\bar{\mathcal{D}}_{\bar{\beta}}\log^{\bar{\beta}}(\lvert x\rvert/x_0+1)$			
$0<H<1/2$	$\propto\log^{2\bar{\beta}}(\sqrt{2}t^H+1)$, Eq. (59)	$\propto\Delta^{2H}$, Eq. (63)	$\propto\frac{\log^{2H(2\bar{\beta}-2)}(T)}{T^{2H}}$, Eq. (64)
$H\geqslant 1/2$	$\propto\log^{2\bar{\beta}}(\sqrt{2}t^H+1)$, Eq. (59)	$\propto\Delta^{2H}$, Eq. (65)	$\propto(1/T)$, Eq. (66)
$G(x)=\bar{\mathfrak{D}}_{\bar{\kappa}}e^{\bar{\kappa}x}$	$\propto e^{2\bar{\kappa}^2t^{2H}}$, Eq. (68)	$\propto\Delta^{2H}$, Eq. (70)	$\propto\frac{e^{2\bar{\kappa}^2T^{2H}}}{T^{2H}}$, Eq. (71)
Time-space-SFBM			
$G(x)=\bar{D}_{\bar{\alpha}}\lvert x\rvert^{\bar{\alpha}}$ for all $F(t)$			
$F(t)=D_\alpha t^\alpha$	$\propto t^{2H\bar{\alpha}\alpha}$, Eq. (89)	$\propto\Delta^{2H}$, Eq. (90)	$\propto T^{2H(\bar{\alpha}\alpha-1)}$, Eq. (91)
$F(t)=\mathcal{D}_\beta\log^\beta(t/\tau+1)$			
$0<H<1/2$	$\propto\log^{2H\bar{\alpha}\beta}(t)$, Eq. (92)	$\propto\Delta^{2H}$, Eq. (94)	$\propto\frac{\log^{2H(\bar{\alpha}\beta-1)}T}{T^{2H}}$, Eq. (95)
$H>1/2$	$\propto\log^{2H\bar{\alpha}\beta}(t)$, Eq. (92)	$\propto\Delta^{2H}$, Eq. (97)	$\propto(1/T)$, Eq. (98)
$F(t)=\mathfrak{D}_\kappa e^{\kappa t}$	$\propto e^{2H\bar{\alpha}\kappa t}$, Eq. (99)	$\propto\Delta^{2H}$, Eq. (100)	$\propto(e^{2H\bar{\alpha}\kappa T}/T)$, Eq. (101)
Subordinated FBM [183]: Nav1.6 diffusion in hippocampal neurons	$\propto t^{0.35}$	$\propto\Delta^{0.81}$	$\propto 1/T^{0.46}$
BM with random diffusivity [184]: receptor motion in living cells	$\propto t^{0.84\pm0.05}$	$\propto\Delta^{0.95\pm0.05}$	$\propto 1/T^{0.17\pm0.05}$
Subordinated FBM [185]: intracellular transport of insulin granules	Not presented	$\propto\Delta^{0.76\ldots0.84}$	$\propto 1/T^{0.2\ldots0.28}$
Random walk with power-law forgetting [186]: time series of word counts in languages	$\propto\log^\alpha(t)$	$\propto\log(\Delta)$	Not presented
Stochastic process of GBM [49,50]: financial time series of stock-market prices	$\propto e^{\sigma^2 t}$	$\propto\Delta^1$	$\propto(e^{\sigma^2T}-1)/T$
Heterogeneous FBM (in time and space) [138]: diffusion of hemocytes of *Drosophila melanogaster*	$\propto t^{1.2\ldots1.5}$	$\propto\Delta^{1.2\ldots1.5}$	Not presented
Subdiffusive CTRW, SBM, or HDPs [133]: ergodicity breaking in silo unclogging via broken arches	$\propto t^{0.4}$	$\propto\Delta^1$	$\propto T^{-0.6}$

level [68,187], in terms of p variation [68], from the first-passage-time [188] and multiscaling [189] perspective, as well as for FBM sheets [190]. The advantage of our current work is the invention of a *general framework* to generate arbitrary time and space clocks for SFBM. It is also the examination of *both* the MSD and the TAMSD (used much more often in SPT) that enabled for the resulting compound process to study the MSD-to-TAMSD nonequivalence and nonergodicity as well as the properties of TAMSD aging.

As examples of applications, time-SBM with a power-law clock was used to describe diffusion in confined nanofilms near a strain-induced critical point [191], and time-SFBM with the Mittag-Leffler clock function to rationalize ultraslow diffusion in porous media [192] (see also Ref. [193]). Diffusion of chloride ions in concrete was also recently accurately described with power-law time-SFBM [194]. FBM with multiscaled clocks was also used, e.g., to mimic diffusion of colloidal particles in microstructural fluids [195]. Interestingly, the extension of FBM [196] with nonlinearly transforming spatial variables was investigated based on a flexible covariance structure and fractal dimension, opening new areas for random-field generation. More general examples where nonstationary processes with nonlinear clocks emerge are, among others, the dynamics of the expanding universe, processes in growing biological cells, non-Fickian dispersion in hierarchically permeable [197,198] multiscale porous media [199–201] for hydrological applications, price fluctuations of stock-market indices in time-varying conditions (e.g., in inflationary scenarios such as in scaled GBM [152]), as well as the dispersion of particles in variably (e.g., with acceleration) aging systems [202].

C. Perspective

From a theoretical viewpoint, as possible directions for future developments of generalized stochastic processes with nonlinear space and time clocks one can propose scenarios of confined and reset time-space-SFBM. For the parental processes, the studies of the potential- and box-confined FBM [125–127], SBM [56], HDPs [89,90], and GBM [203] are available as "landmarks"; the reset versions of FBM [115], SBM [204,205], HDPs [115,206,207], and GBM [52,53] were also examined recently. Additionally, other classes of specific clock functions can be proposed [e.g., piecewise different functional forms of $F(t)$ and $G(x)$] for addressing the physical reality of a given system under investigation.

Finally, *multifractal* [208,209] scenarios of diffusion with, e.g., power-law clocks $F(t)\propto t^{\alpha(t)}$ with time-varying exponent can further be proposed. Moreover, from a data-driven perspective, choosing the most appropriate general stochastic process of SFBM type for a given SPT data set based on the values of the so-called Joseph, Moses, and Noah auxiliary exponents [210,211], computed for the data vs the theory, could offer one more model-assessment criterion, to supplement those based on the MSD and TAMSD scaling relations as well as the TAMSD trace-length dependence (5).

We believe that the process of SFBM will form a good basis for development of advanced machine-learning or Bayesian-inference approaches for *in silico* deciphering of diffusion models behind measured anomalous-diffusion trajectories. Such further developments will move forward the field of generalized stochastic processes used as mathematical tools for description of anomalous-diffusion data.

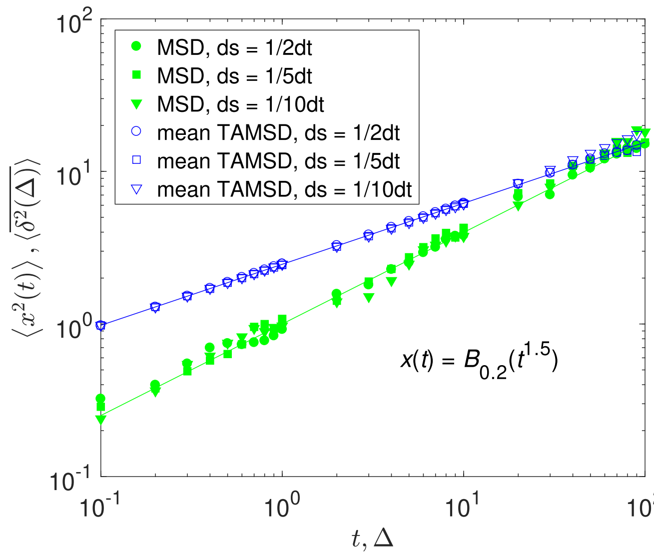

FIG. 12. The same as in Fig. 3 computed for the choices (28) of the time step ds.

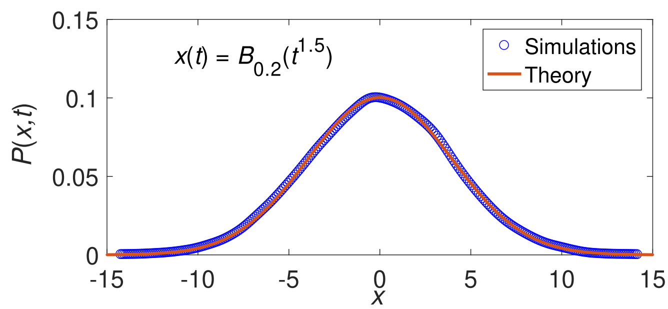

FIG. 13. Simulational (blue circles) and theoretical results (solid red curve) given by Eq. (25) of the PDF for the time-SFBM with (29) at the specific time $t = 100$ for the values of H and α as in Fig. 3.

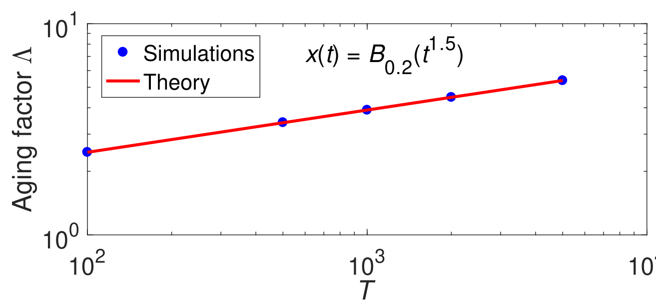

FIG. 14. Simulations (blue circles) and theoretical results (solid curve) given by Eq. (33) for the aging factor Λ for time-SFBM with Eq. (29), for H and α values as in Fig. 3.

ACKNOWLEDGMENTS

We thank Alexey A. Cherstvy for designing Fig. 1. Y.L. acknowledges financial support from the Alexander von Humboldt Foundation (Grant No. 1217531) and the National Natural Science Foundation of China (Grant No. 12372382). R.M. acknowledges financial support from the German Science Foundation (DFG, Grant ME 1535/12-1). A.G.C. thanks S. Thapa and H. Safdari for providing unavailable literature sources.

APPENDIX A: SUPPLEMENTARY FIGURES

Here, we present Figs. 12–32 supporting the claims of the main text.

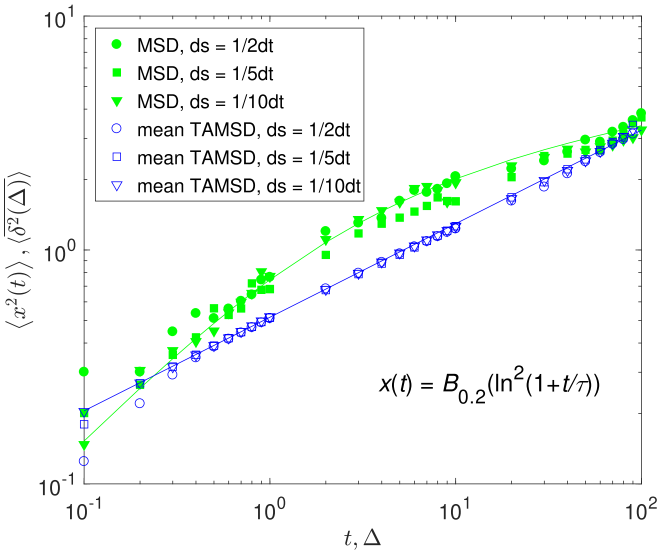

FIG. 15. The same as in Fig. 4 computed for the choices (28) of the time step ds.

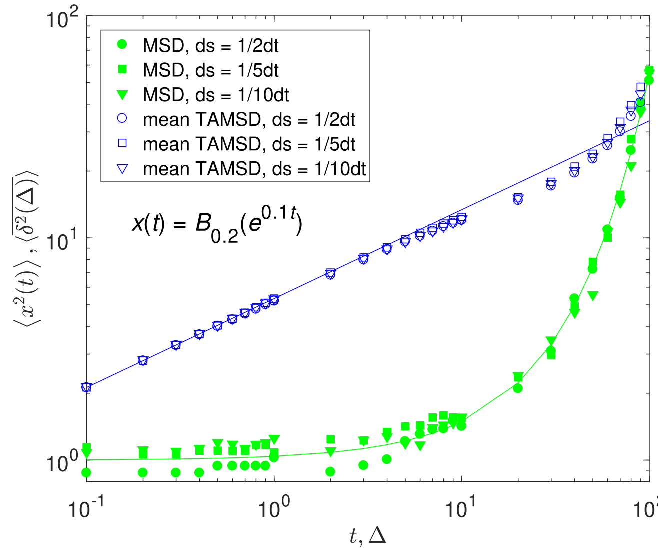

FIG. 18. The same as in Fig. 5 computed for the choices (28) of the time step ds.

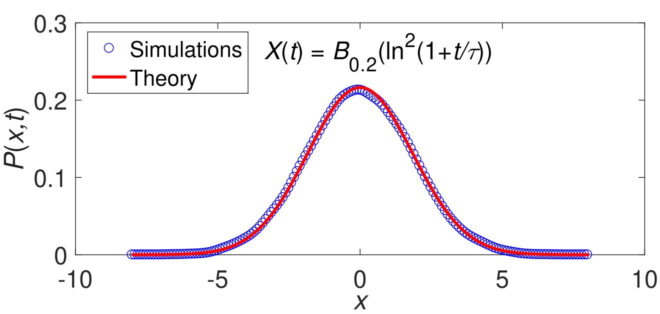

FIG. 16. PDF (25) of time-SFBM with (34) at $t = 100$, computed for H and β as in Fig. 4.

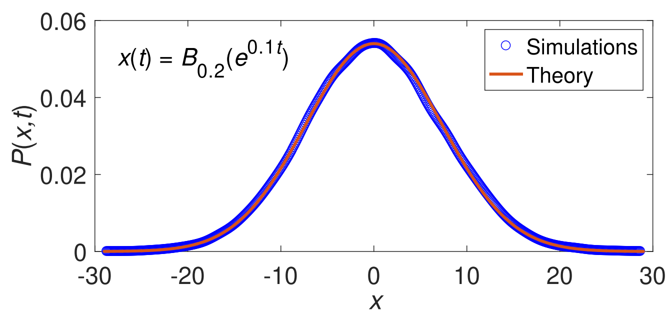

FIG. 19. PDF (25) of time-SFBM with (44) at $t = 100$, for H and κ as in Fig. 5.

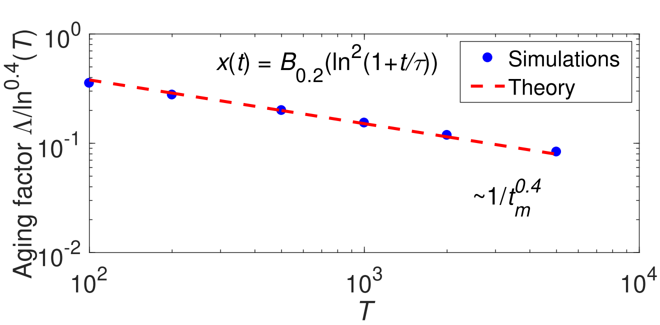

FIG. 17. Aging factor $\Lambda/[\log(T/\tau)]^{2H(\beta-1)}$ [Eq. (39)] of time-SFBM with $F(t)$ [Eq. (34)], shown for the same H and β as in Fig. 4.

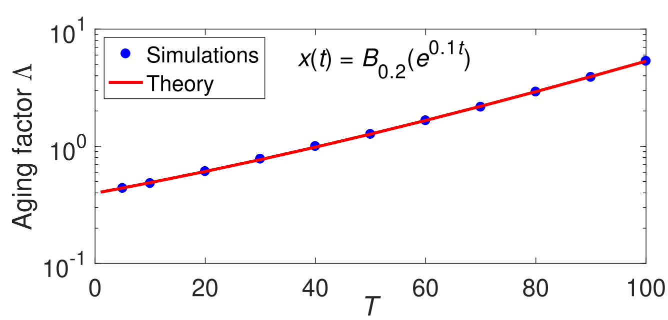

FIG. 20. Aging factor Λ [Eq. (47)] for time-SFBM with (44), for H and κ as in Fig. 5.

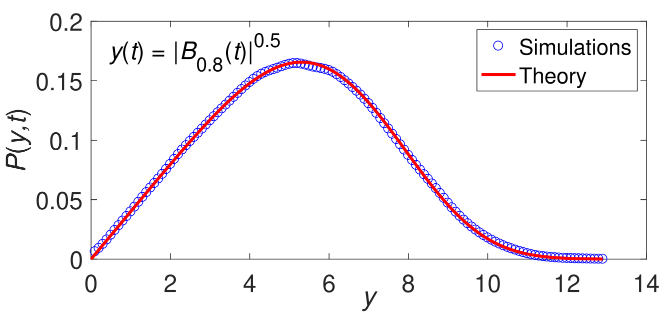

FIG. 21. PDF (55) of space-SFBM with (51) at $t = 100$, computed for H and $\bar{\alpha}$ as in Fig. 6.

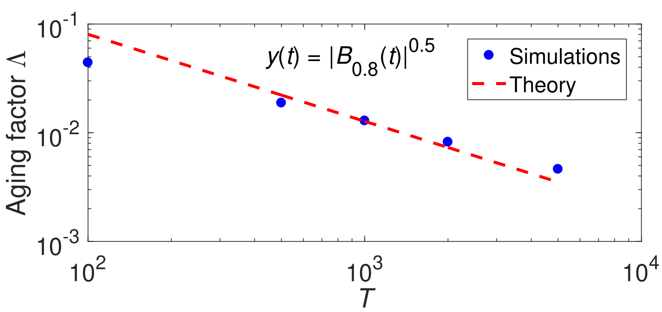

FIG. 22. Aging factor Λ [Eq. (56)] for space-SFBM with (51) for H and $\bar{\alpha}$ as in Fig. 6.

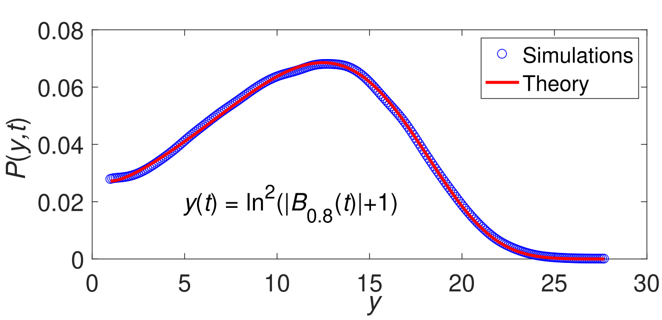

FIG. 23. PDF (55) of space-SFBM with (57) at $t = 100$, computed for H and $\bar{\beta}$ as in Fig. 7.

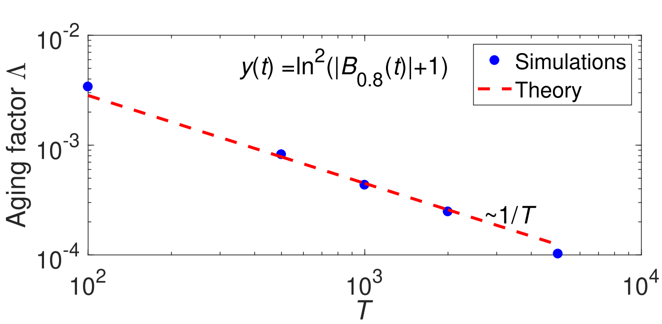

FIG. 24. Aging factor Λ [Eq. (66)] for space-SFBM with (57) for H and $\bar{\beta}$ as in Fig. 7.

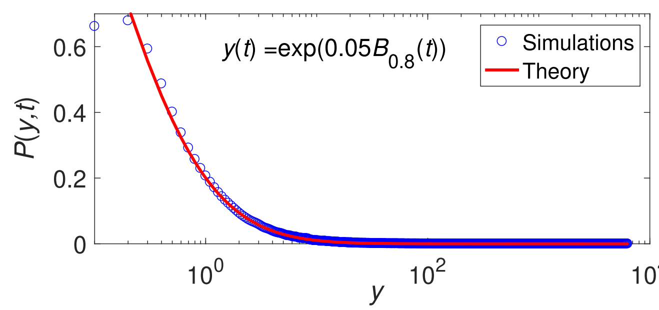

FIG. 25. PDF (69) of space-SFBM with (67) at $t = 100$, computed for H and $\bar{\kappa}$ as in Fig. 8.

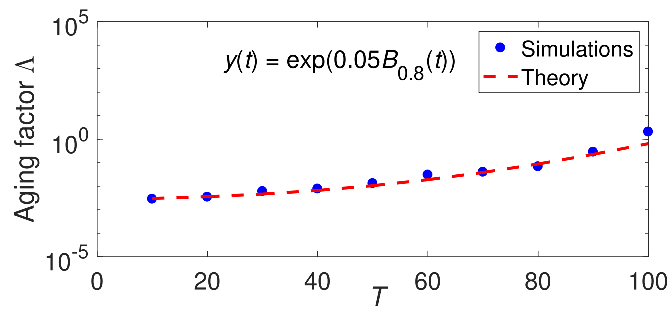

FIG. 26. Aging factor Λ [Eq. (67)] for space-SFBM with (67) for H and $\bar{\kappa}$ as in Fig. 8.

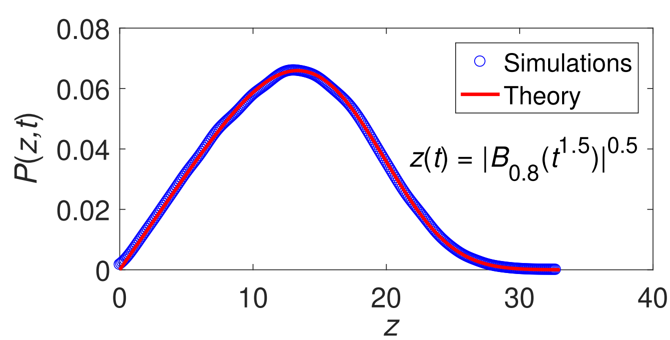

FIG. 27. PDF (74) of time-space-SFBM with (29) and (51) at $t = 100$, computed for H, α, and $\bar{\alpha}$ as in Fig. 9.

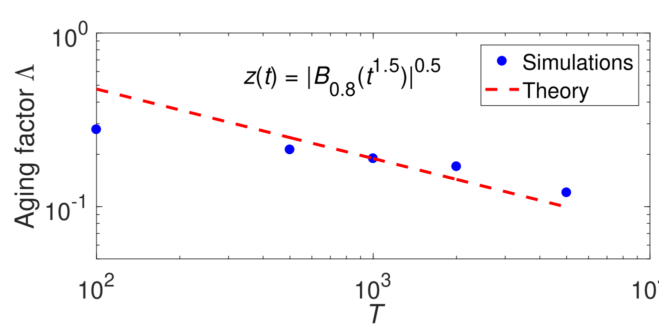

FIG. 28. Aging factor Λ [Eq. (91)] for time-space-SFBM with (29) and (51) for H, α, and $\bar{\alpha}$ as in Fig. 9.

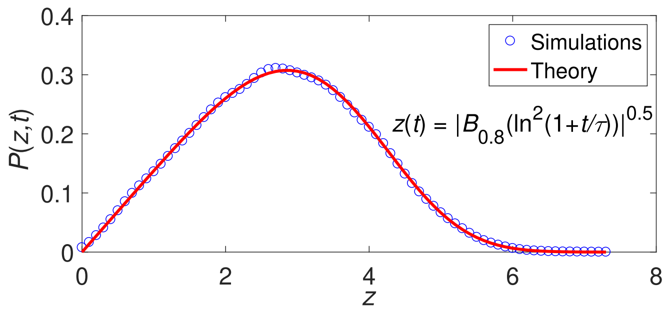

FIG. 29. PDF (74) of time-space-SFBM with (51) and (34) at $t = 100$, computed for H, $\bar{\alpha}$, and β as in Fig. 10.

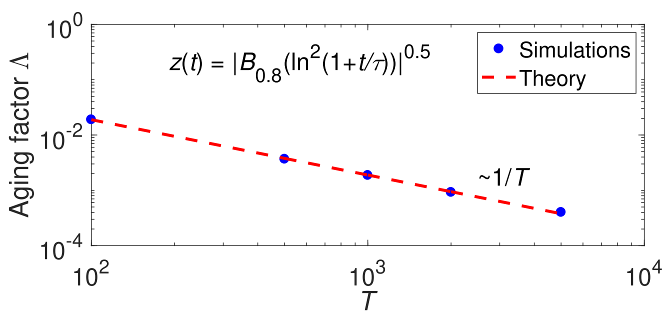

FIG. 30. Aging factor Λ [Eq. (98)] for time-space-SFBM with (51) and (34) for H, $\bar{\alpha}$, and β as in Fig. 10.

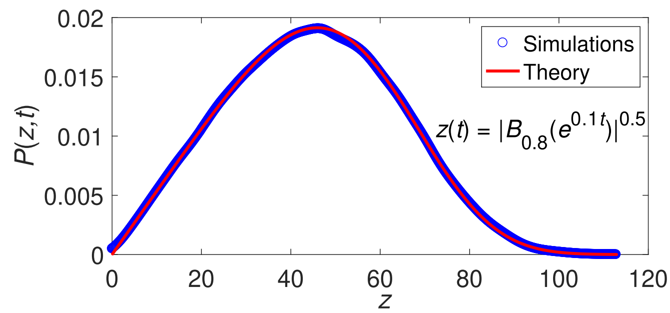

FIG. 31. PDF (74) of time-space-SFBM with (51) and (44) at $t = 100$, computed for H, κ, and $\bar{\alpha}$ as in Fig. 11.

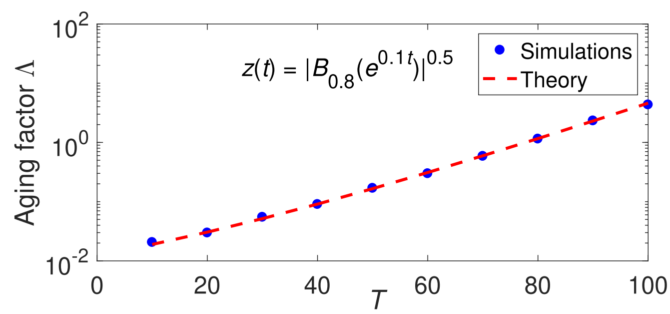

FIG. 32. Aging factor Λ [Eq. (101)] for time-space-SFBM with (51) and (34) for H, κ, and $\bar{\alpha}$ as in Fig. 11.

APPENDIX B: ABBREVIATIONS

Single-particle tracking, SPT; probability-density function, PDF; mean-squared displacement, MSD; time-averaged MSD, TAMSD; Brownian motion, BM; scaled BM, SBM; fractional BM, FBM; scaled FBM, SFBM; geometric BM, GBM; continuous-time random walks, CTRWs; heterogeneous diffusion processes, HDPs.

[1] R. Brown, A brief account of microscopical observations made in the months of June, July and August 1827, on the particles contained in the pollen of plants and on the general existence of active molecules in organic and inorganic bodies, Philos. Mag. **4**, 161 (1828); [Ann. Phys. Chem. **14**, 294 (1828)].
[2] A. Fick, Über Diffusion, Ann. Phys. **170**, 59 (1855).
[3] A. Einstein, Über die von der molekularkinetischen Theorie der Wärme geforderte Bewegung von in ruhenden Flüssigkeiten suspendierten Teilchen, Ann. Phys. **322**, 549 (1905).
[4] A. Einstein, Zur Theorie der Brownschen Bewegung, Ann. Phys. **324**, 371 (1906).
[5] P. Langevin, Sur la theorie du mouvement Brownien, C. R. Seances Acad. Sci. **146**, 530 (1908).
[6] G. E. Uhlenbeck and L. S. Ornstein, On the theory of the Brownian motion, Phys. Rev. **36**, 823 (1930).
[7] S. Chandrasekhar, Stochastic problems in physics and astronomy, Rev. Mod. Phys. **15**, 1 (1943).
[8] L. Boltzmann, Über die Eigenschaften monocyklischer und anderer damit verwandter Systeme, J. Reine Angew. Math. **98**, 68 (1885).
[9] J. L. Lebowitz and O. Penrose, Modern ergodic theory, Phys. Today **26**, 23 (1973).
[10] C. C. Moore, Ergodic theorem, ergodic theory, and statistical mechanics, Proc. Natl. Acad. Sci. USA **112**, 1907 (2015).
[11] S. Burov, R. Metzler, and E. Barkai, Aging and non-ergodicity beyond the Khinchin theorem, Proc. Natl. Acad. Sci. USA **107**, 13228 (2010).
[12] E. Barkai, Y. Garini, and R. Metzler, Strange kinetics of single molecules in living cells, Phys. Today **65**, 29 (2012).
[13] J. H. P. Schulz, E. Barkai, and R. Metzler, Aging Renewal Theory and Application to Random Walks, Phys. Rev. X **4**, 011028 (2014).
[14] R. Metzler, J.-H. Jeon, A. G. Cherstvy, and E. Barkai, Anomalous diffusion models and their properties: Non-stationarity, non-ergodicity, and ageing at the centenary of single particle tracking, Phys. Chem. Chem. Phys. **16**, 24128 (2014).
[15] C. Manzo and M. F. Garcia-Parajo, A review of progress in single particle tracking: From methods to biophysical insights, Rep. Prog. Phys. **78**, 124601 (2015).
[16] C. Bräuchle, D. C. Lamb, and J. Michaelis, *Single Particle Tracking and Single Molecule Energy Transfer* (Wiley-VCH, Weinheim, Germany, 2012).

[17] F. Liu and K. Burrage, Novel techniques in parameter estimation for fractional dynamical models arising from biological systems, Comput. Math. Appl. **62**, 822 (2011).
[18] G. Muñoz-Gil, G. Volpe, M. A. Garcia-March, E. Aghion, A. Argun, C. B. Hong, T. Bland, S. Bo, J. Alberto Conejero, N. Firbas, Ò. Garibo i Orts, A. Gentili, Z. Huang, J.-H. Jeon, H. Kabbech, Y. Kim, P. Kowalek, D. Krapf, H. Loch-Olszewska, M. A. Lomholt, J.-B. Masson, P. G. Meyer *et al.*, Objective comparison of methods to decode anomalous diffusion, Nat. Commun. **12**, 6253 (2021).
[19] H. Seckler and R. Metzler, Bayesian deep learning for error estimation in the analysis of anomalous diffusion, Nat. Commun. **13**, 6717 (2022).
[20] S. Thapa, M. A. Lomholt, J. Krog, A. G. Cherstvy, and R. Metzler, Bayesian nested-sampling analysis of single-particle tracking data: Maximum likelihood for the models of stochastic diffusivity and fractional Brownian motion, Phys. Chem. Chem. Phys. **20**, 29018 (2018).
[21] J. W. Haus and K. W. Kehr, Diffusion in regular and disordered lattices, Phys. Rep. **150**, 263 (1987).
[22] J.-P. Bouchaud and A. Georges, Anomalous diffusion in disordered media: Statistical mechanisms, models and physical applications, Phys. Rep. **195**, 127 (1990).
[23] S. Havlin and D. Ben-Avraham, Diffusion in disordered media, Adv. Phys. **36**, 695 (1987).
[24] R. Metzler and J. Klafter, The random walk's guide to anomalous diffusion: A fractional dynamics approach, Phys. Rep. **339**, 1 (2000).
[25] S. Burov, J.-H. Jeon, R. Metzler, and E. Barkai, Single particle tracking in systems showing anomalous diffusion: The role of weak ergodicity breaking, Phys. Chem. Chem. Phys. **13**, 1800 (2011).
[26] I. M. Sokolov, Models of anomalous diffusion in crowded environments, Soft Matter **8**, 9043 (2012).
[27] Y. Meroz and I. M. Sokolov, A toolbox for determining subdiffusive mechanisms, Phys. Rep. **573**, 1 (2015).
[28] A. A. Tateishi, H. V. Ribeiro, and E. K. Lenzi, The role of fractional time-derivative operators on anomalous diffusion, Front. Phys. **5**, 52 (2017).
[29] H. Sun, Y. Zhang, D. Baleanu, W. Chen, and Y. Chen, A new collection of real world applications of fractional calculus in science and engineering, Commun. Nonlin. Sci. Numer. Simul. **64**, 213 (2018).
[30] V. Sposini *et al.*, Towards a robust criterion of anomalous diffusion, Commun. Phys. **5**, 305 (2022).
[31] E. K. Lenzi *et al.*, A generalized diffusion equation: Solutions and anomalous diffusion, Fluids **8**, 34 (2023).
[32] O. H. E. Philcox and S. Torquato, Disordered Heterogeneous Universe: Galaxy Distribution and Clustering across Length Scales, Phys. Rev. X **13**, 011038 (2023).
[33] A. A. Lagutin and V. V. Uchaikin, Anomalous diffusion equation: Application to cosmic ray transport, Nucl. Instrum. Methods Phys. Res. Sect. B **201**, 212 (2003).
[34] V. V. Uchaikin, Fractional phenomenology of cosmic ray anomalous diffusion, Phys. Usp. **56**, 1074 (2013).
[35] Y. E. Litvinenko, H. Fichtner, and D. Walter, Anomalous transport of cosmic rays in a nonlinear diffusion model, Astrophys. J. **841**, 57 (2017).
[36] M. Weiss, M. Elsner, F. Karberg, and T. Nilsson, Anomalous subdiffusion is a measure for cytoplasmic crowding in living cells, Biophys. J. **87**, 3518 (2004).
[37] F. Etoc, E. Balloul, C. Vicario, D. Normanno, D. Lioe, A. Sittner, J. Piehler, M. Dahan, and M. Coppey, Non-specific interactions govern cytosolic diffusion of nanosized objects in mammalian cells, Nat. Mater. **17**, 740 (2018).
[38] A. Sabri, X. Xu, D. Krapf, and M. Weiss, Elucidating the Origin of Heterogeneous Anomalous Diffusion in the Cytoplasm of Mammalian Cells, Phys. Rev. Lett. **125**, 058101 (2020).
[39] S. Scott, M. Weiss, C. Selhuber-Unkel, Y. F. Barooji, A. Sabri, J. T. Erler, R. Metzler, and L. B. Oddershede, Extracting, quantifying, and comparing dynamical and biomechanical properties of living matter through single particle tracking, Phys. Chem. Chem. Phys. **25**, 1513 (2023).
[40] S. Yui, Y. Tang, W. Guo, H. Kobayashi, and M. Tsubota, Universal Anomalous Diffusion of Quantized Vortices in Ultraquantum Turbulence, Phys. Rev. Lett. **129**, 025301 (2022).
[41] I. Goychuk and Th. Pöschel, Nonequilibrium Phase Transition to Anomalous Diffusion and Transport in a Basic Model of Nonlinear Brownian Motion, Phys. Rev. Lett. **127**, 110601 (2021).
[42] Y. Liang and W. Chen, A non-local structural derivative model for characterization of ultraslow diffusion in dense colloids, Commun. Nonlin. Sci. Numer. Simul. **56**, 131 (2018).
[43] Y. Liang, S. Wang, W. Chen, Z. Zhou, and R. L. Magin, A survey of models of ultraslow diffusion in heterogeneous materials, Appl. Mech. Rev. **71**, 040802 (2019).
[44] P. Rosenau, Fast and Superfast Diffusion Processes, Phys. Rev. Lett. **74**, 1056 (1995).
[45] Y. G. Sinai, The limiting behavior of a one-dimensional random walk in a random medium, Theory Probab. Appl. **27**, 256 (1983).
[46] R. C. Merton, Theory of rational option pricing, Bell J. Econ. Manag. Sci. **4**, 141 (1973).
[47] J. C. Cox and S. A. Ross, The valuation of options for alternative stochastic processes, J. Financ. Econ. **3**, 145 (1976).
[48] J. Clara-Rahola, A. M. Puertas, M. A. Sánchez-Granero, J. E. Trinidad-Segovia, and F. J. de las Nieves, Diffusive and Arrestedlike Dynamics in Currency Exchange Markets, Phys. Rev. Lett. **118**, 068301 (2017).
[49] A. G. Cherstvy, D. Vinod, E. Aghion, A. V. Chechkin, and R. Metzler, Time averaging, ageing and delay analysis of financial time series, New J. Phys. **19**, 063045 (2017).
[50] S. Ritschel, A. G. Cherstvy, and R. Metzler, Universality of delay-time averages for financial time series: Analytical results, computer simulations, and analysis of historical stock-market prices, J. Phys.: Complex. **2**, 045003 (2021).
[51] V. Stojkoski, T. Sandev, L. Basnarkov, L. Kocarev, and R. Metzler, Generalised geometric Brownian motion: Theory and applications to option pricing, Entropy **22**, 1432 (2020).
[52] D. Vinod, A. G. Cherstvy, W. Wang, R. Metzler, and I. M. Sokolov, Nonergodicity of reset geometric Brownian motion, Phys. Rev. E **105**, L012106 (2022).
[53] D. Vinod, A. G. Cherstvy, R. Metzler, and I. M. Sokolov, Nonergodicity of reset geometric Brownian motion with drift, Phys. Rev. E **106**, 034137 (2022).

[54] A. N. Kolmogorov, Wienersche Spiralen und einige andere interessante Kurven im Hilbertschen Raum, C. R. (Dokl.) Acad. Sci. URSS **26**, 115 (1940).

[55] B. B. Mandelbrot and J. W. van Ness, Fractional Brownian motions, fractional noises and applications, SIAM Rev. **10**, 422 (1968).

[56] J.-H. Jeon, A. V. Chechkin, and R. Metzler, Scaled Brownian motion: A paradoxical process with a time dependent diffusivity for the description of anomalous diffusion, Phys. Chem. Chem. Phys. **16**, 15811 (2014).

[57] S. C. Lim and S. V. Muniandy, Self-similar Gaussian processes for modeling anomalous diffusion, Phys. Rev. E **66**, 021114 (2002).

[58] A. G. Cherstvy, A. V. Chechkin, and R. Metzler, Anomalous diffusion and ergodicity breaking in heterogeneous diffusion processes, New J. Phys. **15**, 083039 (2013).

[59] A. G. Cherstvy and R. Metzler, Nonergodicity, fluctuations, and criticality in heterogeneous diffusion processes, Phys. Rev. E **90**, 012134 (2014).

[60] W. Wang, A. G. Cherstvy, X. Liu, and R. Metzler, Anomalous diffusion and nonergodicity for heterogeneous diffusion processes with fractional Gaussian noise, Phys. Rev. E **102**, 012146 (2020).

[61] A. G. Cherstvy and R. Metzler, Ergodicity breaking, ageing, and confinement in generalized diffusion processes with position and time dependent diffusivity, J. Stat. Mech. (2015) P05010.

[62] W. Wang, R. Metzler, and A. G. Cherstvy, Anomalous diffusion, aging, and nonergodicity of scaled Brownian motion with fractional Gaussian noise: Overview of related experimental observations and models, Phys. Chem. Chem. Phys. **24**, 18482 (2022).

[63] A. V. Chechkin, R. Gorenflo, and I. M. Sokolov, Fractional diffusion in inhomogeneous media, J. Phys. A: Math. Gen. **38**, L679 (2005).

[64] Y. He, S. Burov, R. Metzler, and E. Barkai, Random Time-Scale Invariant Diffusion and Transport Coefficients, Phys. Rev. Lett. **101**, 058101 (2008).

[65] R. Hou, A. G. Cherstvy, R. Metzler, and T. Akimoto, Biased continuous-time random walks for ordinary and equilibrium cases: Facilitation of diffusion, ergodicity breaking and ageing, Phys. Chem. Chem. Phys. **20**, 20827 (2018).

[66] W. Deng and E. Barkai, Ergodic properties of fractional Brownian-Langevin motion, Phys. Rev. E **79**, 011112 (2009).

[67] J. H. Cushman, D. O'Malley, and M. Park, Anomalous diffusion as modeled by a nonstationary extension of Brownian motion, Phys. Rev. E **79**, 032101 (2009).

[68] D. O'Malley and J. H. Cushman, Fractional Brownian motion run with a nonlinear clock, Phys. Rev. E **82**, 032102 (2010).

[69] W. Wang, A. G. Cherstvy, A. V. Chechkin, S. Thapa, F. Seno, X. Liu, and R. Metzler, Fractional Brownian motion with random diffusivity: Emerging residual nonergodicity below the correlation time, J. Phys. A: Math. Theor. **53**, 474001 (2020).

[70] W. Wang, F. Seno, I. M. Sokolov, A. V. Chechkin, and R. Metzler, Unexpected crossovers in correlated random-diffusivity processes, New J. Phys. **22**, 083041 (2020).

[71] W. Wang, M. Balcerek, K. Burnecki, A. V. Chechkin, S. Janusonis, J. Slezak, Th. Vojta, A. Wylomanska, and R. Metzler, Memory-multi-fractional Brownian motion with continuous correlations, Phys. Rev. Res. **5**, L032025 (2023).

[72] Y. Liang, W. Wang, and R. Metzler, Anomalous diffusion, non-Gaussianity, and nonergodicity for subordinated fractional Brownian motion with a drift, Phys. Rev. E **108**, 024143 (2023).

[73] S. M. J. Khadem, R. Klages, and S. H. L. Klapp, Stochastic thermodynamics of fractional Brownian motion, Phys. Rev. Res. **4**, 043186 (2022).

[74] A. G. Cherstvy, W. Wang, R. Metzler, and I. M. Sokolov, Inertia triggers nonergodicity of fractional Brownian motion, Phys. Rev. E **104**, 024115 (2021).

[75] B. Meerson, O. Bénichou, and G. Oshanin, Path integrals for fractional Brownian motion and fractional Gaussian noise, Phys. Rev. E **106**, L062102 (2022).

[76] M. Mulansky and A. Pikovsky, Energy spreading in strongly nonlinear disordered lattices, New J. Phys. **15**, 053015 (2013).

[77] A. Hansen, E. G. Flekkoy, and B. Baldelli, Anomalous diffusion in systems with concentration-dependent diffusivity: Exact solutions and particle simulations, Front. Phys. **8**, 519624 (2020).

[78] T. Miyaguchi, T. Uneyama, and T. Akimoto, Brownian motion with alternately fluctuating diffusivity: Stretched-exponential and power-law relaxation, Phys. Rev. E **100**, 012116 (2019).

[79] J. Hull and A. White, The pricing of options on assets with stochastic volatilities, J. Finance **42**, 281 (1987).

[80] M. V. Chubynsky and G. W. Slater, Diffusing Diffusivity: A Model for Anomalous, yet Brownian, Diffusion, Phys. Rev. Lett. **113**, 098302 (2014).

[81] T. Uneyama, T. Miyaguchi, and T. Akimoto, Fluctuation analysis of time-averaged mean-square displacement for the Langevin equation with time-dependent and fluctuating diffusivity, Phys. Rev. E **92**, 032140 (2015).

[82] A. V. Chechkin, F. Seno, R. Metzler, and I. M. Sokolov, Brownian yet Non-Gaussian Diffusion: From Superstatistics to Subordination of Diffusing Diffusivities, Phys. Rev. X **7**, 021002 (2017).

[83] A. Pacheco-Pozo and I. M. Sokolov, Convergence to a Gaussian by Narrowing of Central Peak in Brownian yet Non-Gaussian Diffusion in Disordered Environments, Phys. Rev. Lett. **127**, 120601 (2021).

[84] E. B. Postnikov, A. V. Chechkin, and I. M. Sokolov, Brownian yet non-Gaussian diffusion in heterogeneous media: From superstatistics to homogenization, New J. Phys. **22**, 063046 (2020).

[85] X. Wang and Y. Chen, Ergodic property of random diffusivity system with trapping events, Phys. Rev. E **105**, 014106 (2022).

[86] P. Massignan, C. Manzo, J. A. Torreno-Pina, M. F. García-Parajo, and M. Lewenstein, Nonergodic Subdiffusion from Brownian Motion in an Inhomogeneous Medium, Phys. Rev. Lett. **112**, 150603 (2014).

[87] T. Akimoto and E. Yamamoto, Distributional behavior of diffusion coefficients obtained by single trajectories in annealed transit time model, J. Stat. Mech. (2016) 123201.

[88] A. G. Cherstvy and R. Metzler, Population splitting, trapping, and non-ergodicity in heterogeneous diffusion processes, Phys. Chem. Chem. Phys. **15**, 20220 (2013).

[89] A. G. Cherstvy, A. V. Chechkin, and R. Metzler, Ageing and confinement in non-ergodic heterogeneous diffusion processes, J. Phys. A: Math. Theor. **47**, 485002 (2014).

[90] A. G. Cherstvy, A. V. Chechkin, and R. Metzler, Particle invasion, survival, and non-ergodicity in 2D diffusion

processes with space-dependent diffusivity, Soft Matter **10**, 1591 (2014).
[91] A. G. Cherstvy and R. Metzler, Ergodicity breaking and particle spreading in noisy heterogeneous diffusion processes, J. Chem. Phys. **142**, 144105 (2015).
[92] N. Leibovich and E. Barkai, Infinite ergodic theory for heterogeneous diffusion processes, Phys. Rev. E **99**, 042138 (2019).
[93] X. Wang, W. Deng, and Y. Chen, Ergodic properties of heterogeneous diffusion processes in a potential well, J. Chem. Phys. **150**, 164121 (2019).
[94] A. Bodrova, A. V. Chechkin, A. G. Cherstvy, and R. Metzler, Quantifying non-ergodic dynamics of force-free granular gases, Phys. Chem. Chem. Phys. **17**, 21791 (2015).
[95] A. Bodrova, A. V. Chechkin, A. G. Cherstvy, and R. Metzler, Ultraslow scaled Brownian motion, New J. Phys. **17**, 063038 (2015).
[96] A. G. Cherstvy and R. Metzler, Anomalous diffusion in time-fluctuating non-stationary diffusivity landscapes, Phys. Chem. Chem. Phys. **18**, 23840 (2016).
[97] H. Safdari, A. G. Cherstvy, A. V. Chechkin, A. Bodrova, and R. Metzler, Aging underdamped scaled Brownian motion: Ensemble- and time-averaged particle displacements, nonergodicity, and the failure of the overdamping approximation, Phys. Rev. E **95**, 012120 (2017).
[98] S. B. Yuste, E. Abad, and C. Escudero, Diffusion in an expanding medium: Fokker-Planck equation, Green's function, and first-passage properties, Phys. Rev. E **94**, 032118 (2016).
[99] F. Le Vot, E. Abad, and S. B. Yuste, Continuous-time random-walk model for anomalous diffusion in expanding media, Phys. Rev. E **96**, 032117 (2017).
[100] X. Wang and Y. Chen, Langevin picture of anomalous diffusion processes in expanding medium, Phys. Rev. E **107**, 024105 (2023).
[101] X. Wang, Y. Chen, and W. Wang, Langevin picture of subdiffusion in nonuniformly expanding medium, arXiv:2303.14924.
[102] M. B. Garman and S. W. Kohlhagen, Foreign currency option values, J. Intl. Money Finance **2**, 231 (1983).
[103] J.-P. Bouchaud, Weak ergodicity breaking and aging in disordered systems, J. Phys. I **2**, 1705 (1992).
[104] M. Mangalam and D. G. Kelty-Stephen, Point estimates, Simpson's paradox, and nonergodicity in biological sciences, Neurosci. Biobehav. Rev. **125**, 98 (2021).
[105] M. Mangalam and D. G. Kelty-Stephen, Ergodic descriptors of non-ergodic stochastic processes, J. R. Soc. Interface. **19**, 20220095 (2022).
[106] L. F. Richardson, Atmospheric diffusion shown on a distance-neighbour graph, Proc. R. Soc. London Ser. A **110**, 709 (1926).
[107] G. K. Batchelor, Diffusion in a field of homogeneous turbulence: II. The relative motion of particles, Math. Proc. Camb. Phil. Soc. **48**, 345 (1952).
[108] J. R. Philip, n-diffusion, Aust. J. Phys. **14**, 1 (1961).
[109] B. O'Shaughnessy and I. Procaccia, Analytical Solutions for Diffusion on Fractal Objects, Phys. Rev. Lett. **54**, 455 (1985).
[110] A. W. C. Lau and T. C. Lubensky, State-dependent diffusion: Thermodynamic consistency and its path integral formulation, Phys. Rev. E **76**, 011123 (2007).
[111] P. Kalinay and J. K. Percus, Corrections to the Fick-Jacobs equation, Phys. Rev. E **74**, 041203 (2006).
[112] M. Bauer, A. Godec, and R. Metzler, Diffusion of finite-size particles in two-dimensional channels with random wall configurations, Phys. Chem. Chem. Phys. **16**, 6118 (2014).
[113] E. W. Maby, Bombardment-enhanced diffusion of arsenic in silicon, J. Appl. Phys. **47**, 830 (1976).
[114] J. Kowall, D. Peak, and J. W. Corbett, Impurity-concentration profile for an exponentially decaying diffusion coefficient in irradiation enhanced diffusion, Phys. Rev. B **13**, 477 (1976).
[115] W. Wang, A. G. Cherstvy, H. Kantz, R. Metzler, and I. M. Sokolov, Time averaging and emerging nonergodicity upon resetting of fractional Brownian motion and heterogeneous diffusion processes, Phys. Rev. E **104**, 024105 (2021).
[116] A. Fuliński, Communication: How to generate and measure anomalous diffusion in simple systems, J. Chem. Phys. **138**, 021101 (2013).
[117] F. Thiel and I. M. Sokolov, Scaled Brownian motion as a mean-field model for continuous-time random walks, Phys. Rev. E **89**, 012115 (2014).
[118] A. G. Cherstvy, H. Safdari, and R. Metzler, Anomalous diffusion, nonergodicity, and ageing for exponentially and logarithmically time-dependent diffusivity: Striking differences for massive versus massless particles, J. Phys. D **54**, 195401 (2021).
[119] I. Goychuk and T. Pöschel, Fingerprints of viscoelastic subdiffusion in random environments: Revisiting some experimental data and their interpretations, Phys. Rev. E **104**, 034125 (2021).
[120] M. Weiss, Resampling single-particle tracking data eliminates localization errors and reveals proper diffusion anomalies, Phys. Rev. E **100**, 042125 (2019).
[121] I. Eliazar and T. Kachman, Anomalous diffusion: Fractional Brownian motion vs fractional Ito motion, J. Phys. A: Math. Theor. **55**, 115002 (2022).
[122] J.-H. Jeon and R. Metzler, Fractional Brownian motion and motion governed by the fractional Langevin equation in confined geometries, Phys. Rev. E **81**, 021103 (2010).
[123] J.-H. Jeon and R. Metzler, Inequivalence of time and ensemble averages in ergodic systems: Exponential versus power-law relaxation in confinement, Phys. Rev. E **85**, 021147 (2012).
[124] A. H. O. Wada and T. Vojta, Fractional Brownian motion with a reflecting wall, Phys. Rev. E **97**, 020102 (2018).
[125] T. Vojta, S. Skinner, and R. Metzler, Probability density of the fractional Langevin equation with reflecting walls, Phys. Rev. E **100**, 042142 (2019).
[126] T. Vojta, S. Halladay, S. Skinner, S. Janusonis, T. Gugenberger, and R. Metzler, Reflected fractional Brownian motion in one and higher dimensions, Phys. Rev. E **102**, 032108 (2020).
[127] T. Guggenberger, A. V. Chechkin, and R. Metzler, Absence of stationary states and non-Boltzmann distributions of fractional Brownian motion in shallow external potentials, New J. Phys. **24**, 073006 (2022).
[128] H. Safdari, A. G. Cherstvy, A. V. Chechkin, F. Thiel, I. M. Sokolov, and R. Metzler, Quantifying the non-ergodicity of scaled Brownian motion, J. Phys. A: Math. Theor. **48**, 375002 (2015).
[129] A. G. Cherstvy, O. Nagel, C. Beta, and R. Metzler, Non-Gaussianity, population heterogeneity, and transient superdif-

fusion in the spreading dynamics of amoeboid cells, Phys. Chem. Chem. Phys. **20**, 23034 (2018).
[130] M. Di Pierro, D. A. Potoyan, P. G. Wolynes, and J. N. Onuchic, Anomalous diffusion, spatial coherence, and viscoelasticity from the energy landscape of human chromosomes, Proc. Natl. Acad. Sci. USA **115**, 7753 (2018).
[131] D. S. Novikov, E. Fieremans, S. N. Jespersen, and V. G. Kiselev, Quantifying brain microstructure with diffusion MRI: Theory and parameter estimation, NMR Biomed. **32**, e3998 (2019).
[132] A. G. Cherstvy, S. Thapa, C. E. Wagner, and R. Metzler, Non-Gaussian, non-ergodic, and non-Fickian diffusion of tracers in mucin hydrogels, Soft Matter **15**, 2526 (2019).
[133] B. V. Guerrero, B. Chakraborty, I. Zuriguel, and A. Garcimartín, Nonergodicity in silo unclogging: Broken and unbroken arches, Phys. Rev. E **100**, 032901 (2019).
[134] A. Díez Fernández, P. Charchar, A. G. Cherstvy, R. Metzler, and M. W. Finnis, The diffusion of doxorubicin drug molecules in silica nanoslits is non-Gaussian, intermittent and anticorrelated, Phys. Chem. Chem. Phys. **22**, 27955 (2020).
[135] C. Ayaz, L. Tepper, F. N. Brünig, J. Kappler, J. O. Daldrop, and R. R. Netz, Non-Markovian modeling of protein folding, Proc. Natl. Acad. Sci. USA **118**, e2023856118 (2021).
[136] E. B. Postnikov, A. I. Lavrova, and D. E. Postnov, Transport in the brain extracellular space: Diffusion, but which kind? Int. J. Mol. Sci. **23**, 12401 (2022).
[137] M. Audoin, M. T. Sogaard, and L. Jauffred, Tumor spheroids accelerate persistently invading cancer cells, Sci. Rep. **12**, 14713 (2022).
[138] N. Korabel, G. D. Clemente, D. Han, F. Feldman, T. H. Millard, and T. A. Waigh, Hemocytes in *Drosophila melanogaster* embryos move via heterogeneous anomalous diffusion, Commun. Phys. **5**, 269 (2022).
[139] N. A. Bustos, C. M. Saad-Roy, A. G. Cherstvy, and C. E. Wagner, Distributed medium viscosity yields quasi-exponential step-size probability distributions in heterogeneous media, Soft Matter **18**, 8572 (2022).
[140] C. E. Wagner, M. Krupkin, K. B. Smith-Dupont, Ch. M. Wu, N. A. Bustos, J. Witten, and K. Ribbeck, Biomacromolecules **24**, 628 (2023).
[141] J. Gong, Q. Li, and J. Wang, Anomalous diffusion of optical vortices in random wavefields, arXiv:2303.07690.
[142] T. Song, Y. Choi, J.-H. Jeon, and Y.-K. Cho, Machine learning analysis reveals the dynamics of mode transition in dendritic cell migration, Front. Immunol. **14**, 1129600 (2023).
[143] Kh.-H. Tran-Ba and K. Foreman, Single-molecule tracking of dye diffusion in synthetic polymers: A tutorial review, J. Appl. Phys. **133**, 101101 (2023).
[144] J. Janczura, P. Kowalek, H. Loch-Olszewska, J. Szwabinski, and A. Weron, Classification of particle trajectories in living cells: Machine learning versus statistical testing hypothesis for fractional anomalous diffusion, Phys. Rev. E **102**, 032402 (2020).
[145] H. D. Pinholt, S. S.-R. Bohr, J. F. Iversen, W. Boomsma, and N. S. Hatzakis, Single-particle diffusional fingerprinting: A machine-learning framework for quantitative analysis of heterogeneous diffusion, Proc. Natl. Acad. Sci. USA **118**, e2104624118 (2021).
[146] A. Argun, G. Volpe, and S. Bo, Classification, inference and segmentation of anomalous diffusion with recurrent neural networks, J. Phys. A: Math. Theor. **54**, 294003 (2021).
[147] H. Loch-Olszewska and J. Szwabinski, Impact of feature choice on machine learning classification of fractional anomalous diffusion, Entropy **22**, 1436 (2020).
[148] N. Granik *et al.*, Single-particle diffusion characterization by deep learning, Biophys. J. **117**, 185 (2019).
[149] G. Muñoz-Gil *et al.*, Single trajectory characterization via machine learning, New J. Phys. **22**, 013010 (2020).
[150] S. Thapa, S. Park, Y. Kim, J.-H. Jeon, R. Metzler, and M. A. Lomholt, Bayesian inference of scaled versus fractional Brownian motion, J. Phys. A: Math. Theor. **55**, 194003 (2022).
[151] M. A. F. dos Santos, L. Menon, Jr., and D. Cius, Superstatistical approach of the anomalous exponent for scaled Brownian motion, Chaos Soliton. Fract. **164**, 112740 (2022).
[152] A. G. Cherstvy, D. Vinod, E. Aghion, I. M. Sokolov, and R. Metzler, Scaled geometric Brownian motion features sub- or superexponential ensemble- but linear time-averaged mean-squared displacements, Phys. Rev. E **103**, 062127 (2021).
[153] H. G. E. Hentschel and I. Procaccia, Relative diffusion in turbulent media: The fractal dimension of clouds, Phys. Rev. A **29**, 1461 (1984).
[154] I. Procaccia, Fractal structures in turbulence, J. Stat. Phys. **36**, 649 (1984).
[155] A. Fuliński, Anomalous weakly nonergodic Brownian motions in nonuniform temperatures, Acta Phys. Pol. B **44**, 1137 (2013).
[156] Y. Meroz, I. M. Sokolov, and J. Klafter, Subdiffusion of mixed origins: When ergodicity and nonergodicity coexist, Phys. Rev. E **81**, 010101 (2010).
[157] M. Levin, G. Bel, and Y. Roichman, Measurements and characterization of the dynamics of tracer particles in an actin network, J. Chem. Phys. **154**, 144901 (2021).
[158] X. Wang, Y. Chen, and W. Deng, Strong anomalous diffusion in two-state process with Lévy walk and Brownian motion, Phys. Rev. Res. **2**, 013102 (2020).
[159] J. Liu, P. Zhu, J.-D. Bao, and X. Chen, Strong anomalous diffusive behaviors of the two-state random walk process, Phys. Rev. E **105**, 014122 (2022).
[160] J. Liu, Y. Jin, J.-D. Bao, and X. Chen, Coexistence of ergodicity and nonergodicity in the aging two-state random walks, Soft Matter **18**, 8687 (2022).
[161] A. S. Serov, F. Laurent, Ch. Floderer, K. Perronet, C. Favard, D. Muriaux, N. Westbrook, C. L. Vestergaard, and J.-B. Masson, Statistical tests for force inference in heterogeneous environments, Sci. Rep. **10**, 3783 (2020).
[162] T. Košuta, M. Cullell-Dalmau, F. Cella Zanacchi, and C. Manzo, Bayesian analysis of data from segmented super-resolution images for quantifying protein clustering, Phys. Chem. Chem. Phys. **22**, 1107 (2020).
[163] D. O'Malley, V. V. Vesselinov, and J. H. Cushman, A method for identifying diffusive trajectories with stochastic models, J. Stat. Phys. **156**, 896 (2014).
[164] A. S. Hansen, M. Woringer, J. B. Grimm, L. D. Lavis, R. Tjian, and X. Darzacq, Robust model-based analysis of single-particle tracking experiments with Spot-On, eLife **7**, e33125 (2018).

[165] D. Szarek, Neural network-based anomalous diffusion parameter estimation approaches for Gaussian processes, Int. J. Adv. Eng. Sci. Appl. Math. **13**, 257 (2021).
[166] J. Janczura, M. Balcerek, K. Burnecki, A. Sabri, M. Weiss, and D. Krapf, Identifying heterogeneous diffusion states in the cytoplasm by a hidden Markov model, New J. Phys. **23**, 053018 (2021).
[167] Z. Chen, L. Geffroy, and J. S. Biteen, NOBIAS: Analyzing anomalous diffusion in single-molecule tracks with nonparametric Bayesian inference, Front. Bioinform. **1**, 742073 (2021).
[168] E. A. AL-hada, X. Tang, and W. Deng, Classification of stochastic processes by convolutional neural networks, J. Phys. A: Math. Theor. **55**, 274006 (2022).
[169] J. J. E. Maris, F. T. Rabouw, B. M. Weckhuysen, and F. Meirer, Classification-based motion analysis of single-molecule trajectories using DiffusionLab, Sci. Rep. **12**, 9595 (2022).
[170] H. Verdier, F. Laurent, A. Cassé, C. L. Vestergaard, and J.-B. Masson, Variational inference of fractional Brownian motion with linear computational complexity, Phys. Rev. E **106**, 055311 (2022).
[171] J. A. Kassel, B. Walter, and H. Kantz, Inferring nonlinear fractional diffusion processes from single trajectories, arXiv:2304.02536.
[172] Q. Martinez, C. Chen, J. Xia, and H. Bahai, Sequence-to-sequence change-point detection in single-particle trajectories via recurrent neural network for measuring self-diffusion, Transp. Porous Media **147**, 679 (2023).
[173] O. Vilk, E. Aghion, T. Avgar, C. Beta, O. Nagel, A. Sabri, R. Sarfati, D. K. Schwartz, M. Weiss, D. Krapf, R. Nathan, R. Metzler, and M. Assaf, Unravelling the origins of anomalous diffusion: From molecules to migrating storks, Phys. Rev. Res. **4**, 033055 (2022).
[174] C. Manzo, G. Munoz-Gil, G. Volpe, M. A. Garcia-March, M. Lewenstein, and R. Metzler, Preface: Characterisation of physical processes from anomalous diffusion data, J. Phys. A: Math. Theor. **56**, 010401 (2023).
[175] Courtesy www.pixabay.com for the source images and special thanks to Alexey A. Cherstvy for preparing the artwork.
[176] D. Dieker, Simulation of fractional Brownian motion, Master's thesis, University of Twente, The Netherlands (2004).
[177] J. R. M. Hosking, Modeling persistence in hydrological time series using fractional differencing, Water Resour. Res. **20**, 1898 (1984).
[178] A. T. Wood and G. Chan, Simulation of stationary Gaussian processes in $[0, 1]^d$, J. Comput. Graph. Stat. **3**, 409 (1994).
[179] H. A. Makse, S. Havlin, M. Schwartz, and H. E. Stanley, Method for generating long-range correlations for large systems, Phys. Rev. E **53**, 5445 (1996).
[180] M. Magdziarz and A. Weron, Competition between subdiffusion and Lévy flights: A Monte Carlo approach, Phys. Rev. E **75**, 056702 (2007).
[181] A. Gil, J. Segura, and N. M. Temme, Computing the Kummer function $U(a, b, z)$ for small values of the arguments, Appl. Math. Comput. **271**, 532 (2015).
[182] M. A. Chaudhry and S. M. Zubair, *On a Class of Incomplete Gamma Functions with Applications* (Chapman and Hall/CRC, London, 2001).
[183] Z. R. Fox, E. Barkai, and D. Krapf, Aging power spectrum of membrane protein transport and other subordinated random walks, Nat. Commun. **12**, 6162 (2021).
[184] C. Manzo, J. A. Torreno-Pina, P. Massignan, G. J. Lapeyre, M. Lewenstein, and M. F. Garcia Parajo, Weak Ergodicity Breaking of Receptor Motion in Living Cells Stemming from Random Diffusivity, Phys. Rev. X **5**, 011021 (2015).
[185] S. M. Ali Tabei, S. Burov, H. Y. Kim, A. Kuznetsov, T. Huynh, J. Jureller, L. H. Philipson, A. R. Dinner, and N. F. Scherer, Intracellular transport of insulin granules is a subordinated random walk, Proc. Natl. Acad. Sci. USA **110**, 4911 (2013).
[186] H. Watanabe, Empirical observations of ultraslow diffusion driven by the fractional dynamics in languages, Phys. Rev. E **98**, 012308 (2018).
[187] M. Park and J. H. Cushman, The complexity of Brownian processes run with nonlinear clocks, Mod. Phys. Lett. B **25**, 1 (2011).
[188] D. O'Malley, J. H. Cushman, and G. Johnson, Scaling laws for fractional Brownian motion with power-law clock, J. Stat. Mech. (2011) L01001.
[189] M. Park, D. O'Malley, and J. H. Cushman, Generalized similarity, renormalization groups, and nonlinear clocks for multiscaling, Phys. Rev. E **89**, 042104 (2014).
[190] D. Wu, Fractional Brownian sheets run with nonlinear clocks, J. Math. Phys. **53**, 013514 (2012).
[191] J. H. Cushman, M. Park, and D. O'Malley, A stochastic model for anomalous diffusion in confined nano-films near a strain-induced critical point, Adv. Water Resour. **34**, 490 (2011).
[192] W. Xu, Y. Liang, J. H. Cushman, and W. Chen, Ultrafast dynamics modeling via fractional Brownian motion run with Mittag-Leffler clock in porous media, Int. J. Heat Mass Transf. **151**, 119402 (2020).
[193] W. Xu, Y. Liang, W. Chen, and J. H. Cushman, A spatial structural derivative model for the characterization of superfast diffusion/dispersion in porous media, Int. J. Heat Mass Transf. **139**, 39 (2019).
[194] S. Yan, Y. Liang, and W. Xu, Characterization of chloride ions diffusion in concrete using fractional Brownian motion run with power-law clock, Fractals **30**, 2250177 (2022).
[195] M. Park, J. H. Cushman, and D. O'Malley, Fractional Brownian motion run with a multi-scaling clock mimics diffusion of spherical colloids in microstructural fluids, Langmuir **30**, 11263 (2014).
[196] D. O'Malley, J. H. Cushman, and P. O'Rear, On generating conductivity fields with known fractal dimension and nonstationary increments, Water Resour. Res. **48**, W03201 (2012).
[197] J. H. Cushman and T. R. Ginn, Nonlocal dispersion in media with continuously evolving scales of heterogeneity, Transp. Porous Media **13**, 123 (1993).
[198] A. Puyguiraud, Ph. Gouze, and M. Dentz, Pore-Scale Mixing and the Evolution of Hydrodynamic Dispersion in Porous Media, Phys. Rev. Lett. **126**, 164501 (2021).
[199] S. P. Neuman and D. M. Tartakovsky, Perspective on theories of non-Fickian transport in heterogeneous media, Adv. Water Resour. **32**, 670 (2009).
[200] I. Battiato, D. M. Tartakovsky, A. M. Tartakovsky, and T. D. Scheibe, Hybrid models of reactive transport in porous and fractured media, Adv. Water Resour. **34**, 1140 (2011).
[201] J. H. Cushman, *The Physics of Fluids in Hierarchical Porous Media: Angstroms to Miles* (Kluwer Academic, Boston, 1997).

[202] M. Bernaschi, A. Billoire, A. Maiorano, G. Parisi, and F. Ricci-Tersenghi, Strong ergodicity breaking in aging of mean-field spin glasses, Proc. Natl. Acad. Sci. USA **117**, 17522 (2020).
[203] D. Veestraeten, Currency option pricing in a credible exchange rate target zone, Appl. Financ. Econ. **23**, 951 (2013).
[204] A. S. Bodrova, A. V. Chechkin, and I. M. Sokolov, Nonrenewal resetting of scaled Brownian motion, Phys. Rev. E **100**, 012119 (2019).
[205] A. S. Bodrova, A. V. Chechkin, and I. M. Sokolov, Scaled Brownian motion with renewal resetting, Phys. Rev. E **100**, 012120 (2019).
[206] T. Sandev, V. Domazetoski, L. Kocarev, R. Metzler, and A. V. Chechkin, Heterogeneous diffusion with stochastic resetting, J. Phys. A: Math. Theor. **55**, 074003 (2022).
[207] W. Wang, A. G. Cherstvy, R. Metzler, and I. M. Sokolov, Restoring ergodicity of stochastically reset anomalous-diffusion processes, Phys. Rev. Res. **4**, 013161 (2022).
[208] H. E. Stanley and P. Meakin, Multifractal phenomena in physics and chemistry, Nature (London) **335**, 405 (1988).
[209] Z.-Q. Jiang, W.-J. Xie, W.-X. Zhou, and D. Sornette, Multifractal analysis of financial markets: A review, Rep. Prog. Phys. **82**, 125901 (2019).
[210] Ph. G. Meyer, V. Adlakha, H. Kantz, and K. E. Bassler, Anomalous diffusion and the Moses effect in an aging deterministic model, New J. Phys. **20**, 113033 (2018).
[211] E. Aghion, Ph. G. Meyer, V. Adlakha, H. Kantz, and K. E. Bassler, Moses, Noah and Joseph effects in Lévy walks, New J. Phys. **23**, 023002 (2021).